

Copyright © 1989, by the author(s).
All rights reserved.

Permission to make digital or hard copies of all or part of this work for personal or classroom use is granted without fee provided that copies are not made or distributed for profit or commercial advantage and that copies bear this notice and the full citation on the first page. To copy otherwise, to republish, to post on servers or to redistribute to lists, requires prior specific permission.

**EFFECTS OF EXCIMER LASER RADIATION
PROPERTIES ON CONDENSER ILLUMINATION
FOR MICROLITHOGRAPHY**

by

William Partlo

Memorandum No. UCB/ERL M89/68

25 May 1989

cover MCE

**EFFECTS OF EXCIMER LASER RADIATION
PROPERTIES ON CONDENSER ILLUMINATION
FOR MICROLITHOGRAPHY**

by

William Partlo

Memorandum No. UCB/ERL M89/68

25 May 1989

ELECTRONICS RESEARCH LABORATORY

College of Engineering
University of California, Berkeley
94720

**EFFECTS OF EXCIMER LASER RADIATION
PROPERTIES ON CONDENSER ILLUMINATION
FOR MICROLITHOGRAPHY**

by

William Partlo

Memorandum No. UCB/ERL M89/68

25 May 1989

ELECTRONICS RESEARCH LABORATORY

College of Engineering
University of California, Berkeley
94720

**Effects of Excimer Laser Radiation Properties on Condenser
Illumination for Microlithography**

William Partlo

Department of Electrical Engineering and Computer Sciences

University of California, Berkeley, California 94720, U.S.A.

ABSTRACT

Use of line-narrowed excimer lasers as a source for microlithography presents problems for illuminator design. The narrow spectral width and high degree of collimation of excimer laser radiation create interference effects in illuminator systems which degrade the uniformity of the illumination produced. In this project, the properties of a line-narrowed excimer laser are measured and their effects on illuminator systems are studied.

May 20, 1989

Dedication

This master's report is dedicated to my parents. They took a little kid who liked to play in the dirt and sent him off to school.

Acknowledgements

I would like to thank my research adviser, Professor William G. Oldham, for his support and assistance during this project. His financial, and more importantly, intellectual generosity made this project possible. I would also like to thank Professor Andrew R. Neureuther for his valuable comments.

Several students, without their help this project would have been impossible, deserve great thanks. Gino Addiego's excellent practical knowledge in the field of optics has been most helpful. Without the thankless help in the microlab from Don Lyons, I would still be in there now. Candid discussions with Chris Spence have help steer me away from unproductive paths. Many other students, namely Carl Galewski, Pantas Sutardja, Kenny Toh, Edward Scheckler, Rich Ferguson, and Nelson Tam have been most helpful. I would also like to thank Richard Hsu for his assistance.

Financial support for this project is provided by the Semiconductor Research Corporation, SEMATECH, and the California MICRO program.

Table of Contents

Dedication	i
Acknowledgements	ii
Table of contents	iii
Chapter 1: Introduction	
1. Motivation	1
2. Previous Experimental Work	1
3. Project Overview	2
4. References	3
Chapter 2: Experimental Equipment	
1. Excimer Laser	4
2. Two Dimensional Imaging Array System	7
3. Linear Array Reticon System	8
4. Average Power and Pulse Energy Detectors	9
5. Vibration Isolation Table	9
6. References	11
7. Figures	12
Chapter 3: Excimer Laser Characteristics	
1. Average Power and Pulse Energy	17
2. Beam Profile	17
3. Beam Divergence	20
4. Spectral Linewidth	21

5. Coherence Length	22
6. References	23
7. Figures	24
Chapter 4: Illuminator Components	
1. Square Light Pipe	33
2. Hexagonal Light Pipe	35
3. BOLD Illuminator (Rotating Diffuser)	35
4. References	38
5. Figures	39
Chapter 5: Conclusion	48
Appendix A: Laser Gas Change Details	49
Appendix B: Camera and Laser Synchronization	51

Chapter 1: Introduction

1. Motivation

The use of shorter wavelengths for illumination in microlithography gives improved performance by reducing the fundamental limit of minimum printable feature size. Historically, strong radiation lines from high pressure mercury bulbs were used as the radiation source in lithographic tools. Most optical glasses become opaque in the deep UV region of the spectrum. Only one material, quartz, has appropriate transmission properties and is robust enough for use in lithography lenses. Lenses crafted from a single optical material cannot be designed to eliminate the chromatic aberrations caused by the natural dispersion of glass.

Because deep UV lenses do not possess any color correction, the illuminating radiation used must have a very small spectral width. Lenses built for current deep UV steppers require a spectral width of not more than 5 nm. Mercury bulbs cannot provide sufficient energy in such a narrow spectral width. Hence, the need for excimer lasers. Line narrowed excimer lasers provide high optical power with narrow spectral width at wavelengths suitable for deep UV lithography. The laser used in these experiments is a KrF excimer which lases at a nominal wavelength of 248.4 nm.

2. Previous Experimental Work

Workers at AT&T Bell Labs first designed and constructed a excimer-based deep UV stepper in 1986¹. Their results clearly showed the viability of excimer-based steppers. They also found the major drawback to be the coherent noise created by the interaction of the excimer radiation's coherence properties with the components used in the system's optical train. The analysis of this problem was further advanced by workers at NTT LSI Laboratories². Their investigation made a broad connection between interference effects

in illuminators and the spatial and temporal coherence of the excimer source.

3. Project Overview

All of the above mentioned work concentrated on the lithography system as a whole. The contribution to fringe production by individual components in the system was not investigated. This project will attempt to measure the interference effects created by various components used in common illuminator systems. Chapter 2 describes and explains the equipment used in these experiments. The excimer laser's pertinent characteristics are discussed in chapter 3. These are average energy, beam profile, beam divergence, spectral width, and coherence length. The theoretical relationship between spectral width and coherence length will also be verified. Finally, chapter 4 will give the results of measurements made on several illuminator components and systems.

4. References

1. Victor Pol, et. al., "Excimer Laser-Based Lithography: A Deep Ultraviolet Wafer Stepper," *Proc. of SPIE on Optical Microlithography V*, vol. 633, pp. 6-16, March 1986.
2. Yoshiharu Ozaki, et. al., "Effect of Temporal and Spatial Coherence of Light Source on Patterning Characteristics in KrF Excimer Laser Lithography," *Proc. of SPIE Optical/Laser Microlithography*, vol. 922, pp. 444-448, March 1988.

Chapter 2: Experimental Equipment

1. Excimer Laser

The excimer laser is a recent entry into the field of lasers with truly industrial capability. The term excimer is used to describe a dimer which is bound in an excited state and dissociated in the unexcited or ground state. The first excimer system was proposed in 1966 by N.G. Basov, but not constructed until 1970^{1 2}. The first commercial excimer laser system was introduced in 1975.

1.1. Laser Specifications

The Excimer laser used in this project is manufactured by Cymer Laser Technologies and is the line-narrowed version of the CX-2 series. The lasing gas is KrF, which lases at a nominal wavelength of 248nm. The line-narrowing of this laser will be discussed later. The laser's pertinent specifications are listed in table 2.1³. The 3 watts average power is typical for lasers installed in excimer based microlithography tools at this time.

As mentioned in the introduction, the spectral width of 3 pm is required due to the lack of chromatic correction in the deep UV lenses used in excimer steppers. The total spectral width acceptable for these lenses is typically 5 pm. The remaining 2 pm of allowed bandwidth is necessary for long term frequency drift of the laser's center line.

1.2. Laser Placement

The excimer laser is located in the U.C. Berkeley Microlab. Due to the laser's large physical size, it is mounted on a table in the service chase adjacent to a class 100 clean room. The general layout of the service chase and the clean room is shown in Fig. 2.2. A safety gas cabinet contains the two cylinders of gas used for the laser and all the plumbing needed to supply these gases to the laser. The vacuum pump and plumbing used to remove the expended laser gas is located under the laser table in the service chase.

The laser beam is diverted by three mirrors into the clean room. These three mirrors comprise a beam steering system which allows for adjustment of the height and angle of the beam as it enters the clean room. The height and direction of the beam could be adjusted with the use of only two mirrors, but the beam would then enter the clean room rotated by ninety degrees. This would make the beam wider than it is high. Turning mirrors on the optical table would vignette the beam since they present greater usable height than width. This vignetting problem is demonstrated in Fig. 2.3. The two situations are shown, the laser traveling tall and narrow, and the laser traveling short and wide. Clearly the first situation is superior.

The beam steering mirrors in the service chase are two inches in diameter so that no vignetting occurs in the service chase. A small plate with a grid of $\frac{1}{4}$ -20 tapped holes spaced by one inch is mounted directly in front of the laser to facilitate experiments which must be performed directly at the laser head.

1.3. Gas Handling System

Fig. 2.4 shows the cylinders and plumbing inside the gas cabinet. The cylinder on the left is 99.999% pure helium used for purging the laser and all tubing before each gas fill. The cylinder on the right is 1.0% Krypton, 0.1% Fluorine, and the balance neon. Valves V1 and V2 are used in the refilling procedure. Valves V3 and V4 are used for purging when a new cylinder is installed.

Fig. 2.4 also shows the plumbing located under the laser table. Valve V5 is used to bypass the laser inlet and outlet for purging. Valve V6 connects the vacuum pump to the system and V7 is used to bleed off excess pressure from the system through the check valve. Finally V8 is used during a cylinder change and V9 is used during an oil trap bake.

Appendix A contains the details for changing the laser gas.

1.4. Laser Operation

The excimer laser can be operated either from its own control paddle or via a standard RS232 serial interface. From cold start up the laser goes through a 15 minute warm up cycle during which the high voltage thyatron is brought to its operating temperature. After completing the warm up cycle, the laser enters STANDBY mode. At the STANDBY level, the laser voltage, energy, pulse rate, and burst number can be adjusted. The final level of operation is LASER ON. The laser must be at the LASER ON level and receive a fire trigger signal before it will emit radiation.

There are two methods of triggering the laser. The first method is called gated mode. In this mode the trigger signal originates from the control paddle. The second method is called triggered mode and the trigger signal originates external to the laser. This mode is useful for synchronizing the laser to other equipment. The two dimensional camera system makes use of the external trigger signal to synchronize the laser pulse with the camera frame read out.

1.5. Laser Line-narrowing Package

The excimer laser is equipped with a package of optics in place of the rear cavity mirror which narrows the spectral width of the radiation emitted from the laser. This package consists of a grating and several beam expansion optics. The use of a grating to line-narrow the laser is one of several possible methods of line-narrowing excimer lasers. Other methods include the use of etalons, prisms, and combinations of these dispersive elements⁴. The grating disperses the radiation while reflecting back into the cavity. Only the most parallel of the reflected rays survive the round trip travel and are amplified by the laser medium and thus the emitted radiation is spectrally narrowed. The grating is mounted on a stepper motor so that the grating can be rotated to choose the laser's center

line.

2. Two Dimensional Imaging Array System

Ordinary optical glass will not transmit 248nm radiation. The human eye is not sensitive to this radiation. The problem of detecting the excimer light is not a trivial one. Most glasses are fluorescent in the visible when exposed to deep UV radiation. Ordinary photographic paper after exposure and development also has excellent fluorescence properties. Each is quite sensitive and useful for general beam alignment. The major drawbacks of these materials are their lack of resolution and their inability to make a permanent recording of the incident image. A two dimensional silicon detector is a flexible solution to this problem.

2.1. System Specifications

The system used in this project is manufactured by Big Sky Software Corp. The system consists of a General Electric TN2509 solid state camera and an IBM AT computer controller. The camera has 253 vertical by 260 horizontal pixels each on 28 μm centers. The camera does not have any published data for its sensitivity at 248nm. The camera has a quartz faceplate so that its spectral response should be that of silicon itself. The controller system has 4MB of RAM and can store 32 full-resolution pictures or 64 half-resolution pictures.

2.2. Camera-Laser Synchronization

A small digital circuit is required to condition the synchronization signals between the camera and the laser. This circuit is shown in Fig. 2.5. The theory of operation and other details of this circuit are given in appendix B. This circuit also gives us the ability to perform multiple pulse integration on up to 255 laser pulses. Integration is helpful for very low light levels, such as the Fabry-Perot interferometer described later. Integration

also improves imaging when the incident light contains random noise which varies from pulse to pulse. The laser's beam profile possesses some random fluctuation which is smoothed out during integration.

3. Linear Array Reticon System

Some applications require imaging in only one dimension. The most obvious experiment needing a linear array is the spectrometer used to measure line center stability. Another experiment which makes use of the linear array is measurement of the beam divergence.

3.1. System Specifications

The linear array used in these experiments is a 1024 pixel, silicon-based Reticon. The pixels are 25 μm wide and 2.5 mm high. The Reticon, like the camera, has a quartz faceplate to facilitate the detection of deep UV radiation. The reticon has a built in cooling system based on the Peltier effect. The detector can be cooled to -55 degrees centigrade. This low temperature reduces the thermal noise generated during long integration times. Coolant water must be supplied to remove waste heat. The detector must also be purged with nitrogen or held under vacuum to prevent condensation on the faceplate.

3.2. Reticon-Laser Synchronization

Synchronizing the linear array and the laser is considerably easier than the camera and laser. The reticon can be operated in four triggering modes, only two of which are of interest to this project. The first and most straight forward is free running mode. In this mode, the reticon is scanned up to 30 times a second and is synchronized with the power line. This mode is useful when measuring continuous sources such as the low pressure mercury bulb used for calibration of the spectrometer. For low light levels, the scan rate can be slowed to as slow as one scan every 1000 seconds.

The second method of triggering is called external sync mode. In this mode, a scan is initiated by the rising edge of a signal supplied externally. Trigger signals received during a scan are ignored, so the laser pulse rate must be kept at or below 30 pps. One drawback with this method is the fact that the reticon integrates all light while waiting for the external trigger signal. If the laser is pulsed too slowly a high level of background will be accumulated in the detector.

4. Average Power and Pulse Energy Detectors

Both the average power and pulse energy detectors used in this project are based on the principle of converting the electro-magnetic energy of the laser light into thermal energy. The pulse energy detector consists of a single thermoelectric junction which absorbs the laser light and converts its energy into a voltage pulse. The peak of this voltage pulse gives the energy, in joules, of a single laser pulse. The minimum measurable energy is 10 mj. This detector is limited to a repetition rate of 10 pps due to thermal time constants.

The average power meter uses a stack of thermoelectric junctions to measure the steady state temperature difference between the detector head and a large thermal mass kept at constant temperature. This temperature difference gives a measure of the average power absorbed by the detector head. This detector has no upper limit on repetition rate and has a 0.5 pps lower limit. The minimum detectable energy is 2 mW.

5. Vibration Isolation Table

Several experiments in this project require extremely stable positioning. The Michelson interferometer must maintain mirror positioning to fractions of a wavelength. The vibrations coupled from the microlab floor onto the optical table move the mirrors several wavelengths. The air suspension legs on the optical table decouple the table's surface from the floor and reduce the mirror vibrations to a tolerable level.

A practical problem with the air isolation is leveling the table surface. Each time the load on the table is changed the pressure in each leg is automatically adjusted to return the table surface to its original position. This scheme works well to within approximately 0.5 mm. Since the laser is not mounted on the optical table, the laser beam goes out of adjustment relative to the optical table's surface each time the load on the table is changed.

6. References

1. N. G. Basov, "Opening Remarks: Fourth International Quantum Electronics Conference," *IEEE J. Quantum Electronics*, vol. QE-2, no. 9, pp. 354-356, Sept. 1966.
2. N.G. Basov, et al., "Laser Operating in the Vacuum Region of the Spectrum by Excitation of Liquid Xenon with an Electron Beam," *JETP Letters*, vol. 12, pp. 329-331, Nov. 1970.
3. R.L. Sandstrom, R.P. Akins, U. Sengupta, "Krypton Fluoride Excimer Laser for Microlithography," *Proc. of SPIE on Optical/Laser Microlithography*, vol. 992, pp. 450-453, Mar. 1989.
4. T.A. Znotins, et al., "The Design of Excimer Lasers for use in Microlithography," *Proc. of SPIE on Optical/Laser Microlithography*, vol. 922, pp. 454-460, Mar. 1988.

CX-2LS Specifications		
	Value	Units
Wavelength	248.4	nm
Spectral Bandwidth (FWHM)	3	pm
Long Term Freq. Drift	±0.5	pm
Average Power @ 200 Hz	3	Watts
Maximum Pulse Energy	20	mJ
Maximum Repetition Rate	250	Hz
Pulse Duration (FWHM)	20	ns
Beam Dimensions (V X H)	17.5 X 7	mm
Beam Divergence (V X H)	2.6 X 3.5	mrad
Pulse-to-Pulse Energy Variation	±5	percent
Gas lifetime @ 3 watts/200 Hz	8	hours
Voltage Requirements	208	VAC
Power Requirements	3	kVA
Water Cooling	4	liter/min.
Gas Volume	90	liter atm.
Nitrogen Purge	10	liter/hour

Table 2.1. Cymer CX-2LS Specifications.

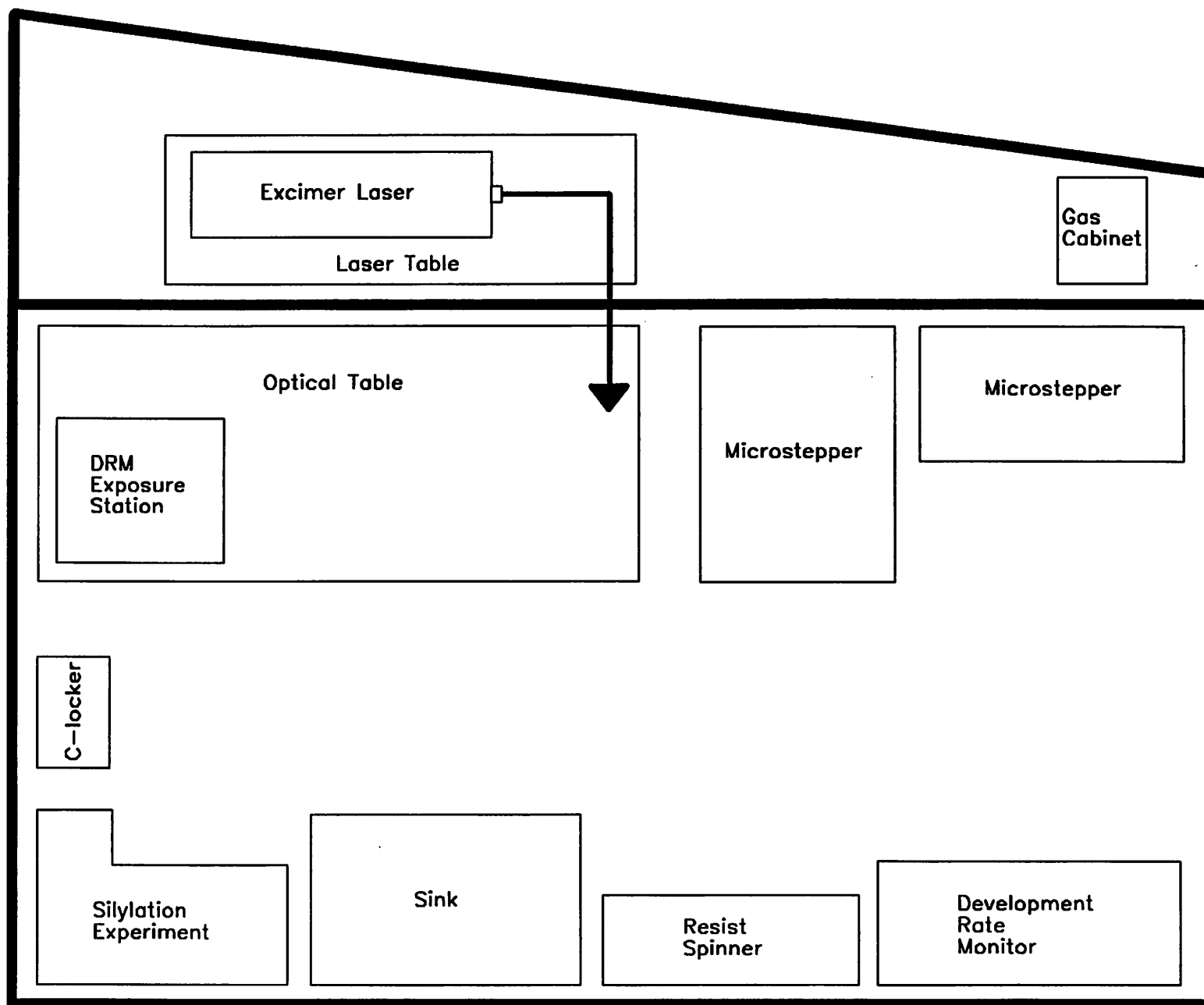


Fig. 2.2 Room Layout.

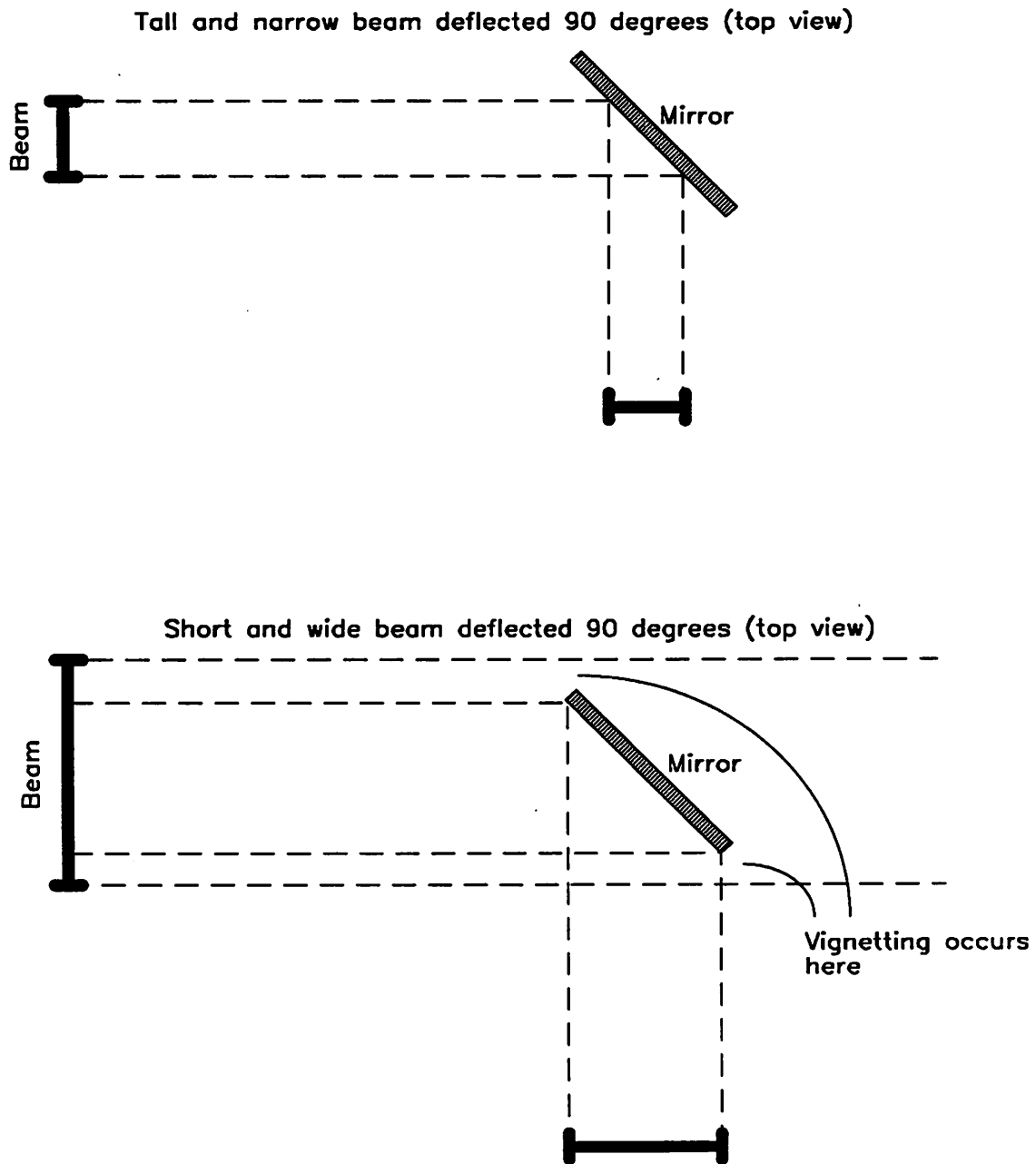


Fig. 2.3 Reduction of vignetting with proper beam orientation.

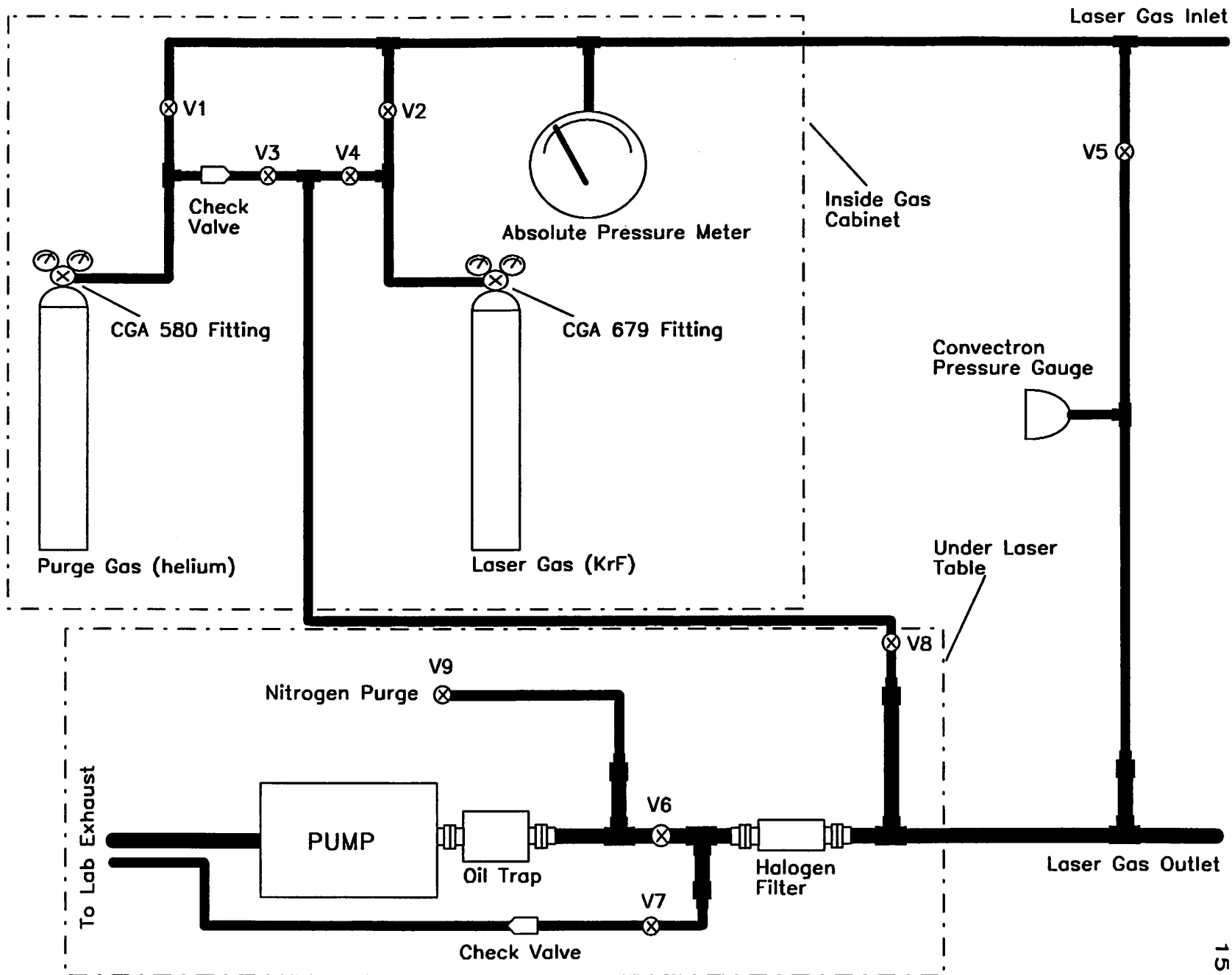


Fig. 2.4 Laser gas handling system.

Signals from and to Camera System

Signals from and to Laser

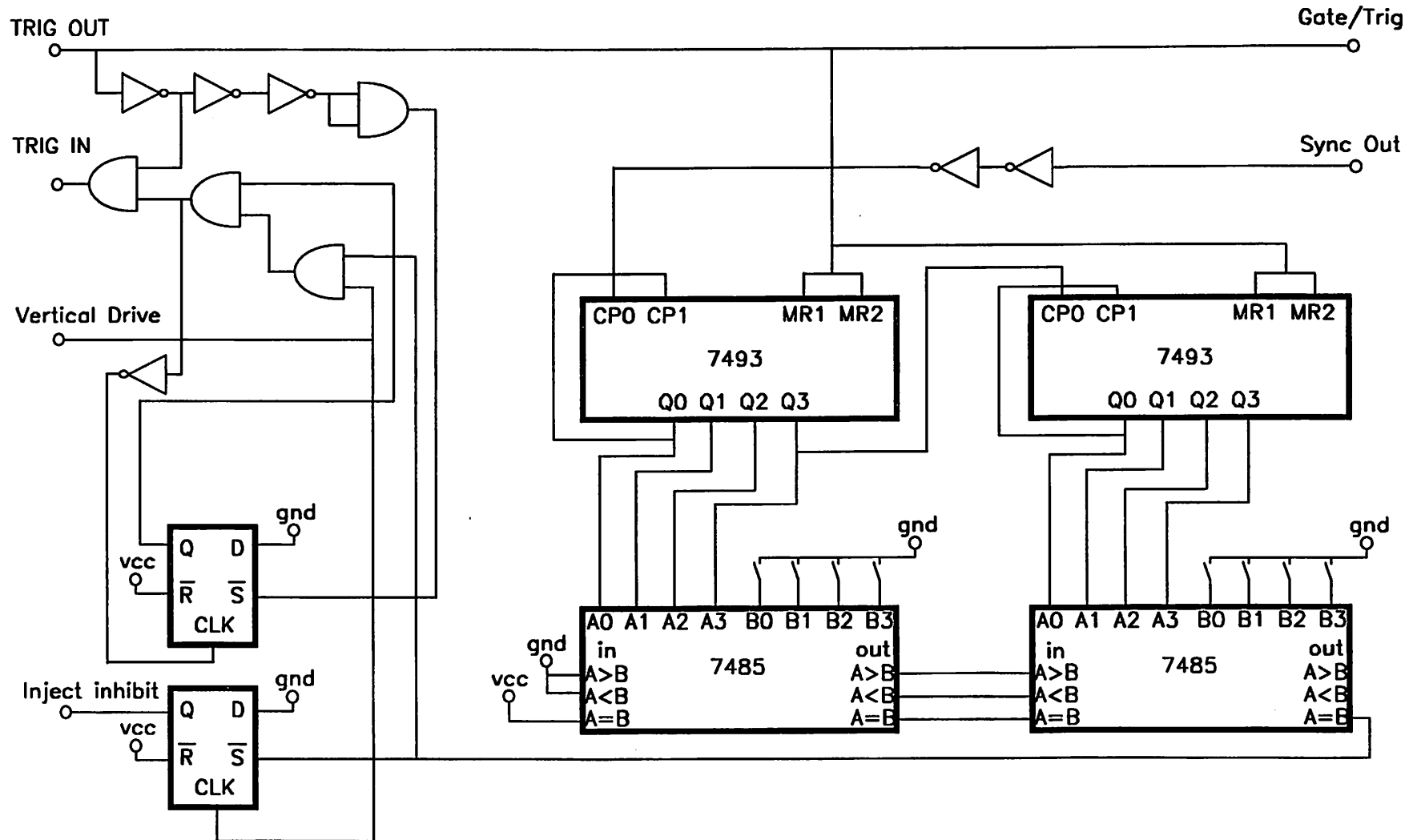


Fig. 2.5 Camera-laser synchronization circuit

Chapter 3: Excimer Laser Characteristics

1. Average Power and Pulse Energy

Following a fresh gas fill, the average output power increases for about 30 minutes until reaching its peak power. The premixed KrF gas used in these experiments is too rich in fluorine and each new run with fresh gas must burn off some of the excess fluorine. A typical gas fill will last for 8 hours of continuous operation. Fig. 3.1 shows power versus time for the line-narrowed laser with a fresh gas fill. The laser was operated at 200 pps with a fixed electrode voltage of 15.5 kv. The output power was measured with a Scientech average power meter placed directly in front of the laser output window.

The laser may also be operated in constant energy mode. In this mode the laser measures the output energy and adjusts the electrode voltage to attain a prescribed output. Fig. 3.2 shows the laser's average power versus time in constant energy mode. A pulse energy of 15mj/pulse was requested with a pulse rate of 200 pps. This gives an average power of 3 watts.

2. Beam Profile

Unlike many other conventional lasers, the beam profile of an excimer laser is not a gaussian shape. The existence of more than one longitudinal mode in a laser beam is common for many lasers. These modes correspond to the Fabry-Perot etalon resonant frequencies which fall inside the gain envelope of the lasing gas. The excimer departs from common lasers in that it also possesses more than one transverse mode. These different transverse modes vary in intensity distribution across the beam profile.

2.1. Cavity Modes

One can estimate the number of modes present in the an excimer beam by taking a simple cubic resonator with dimensions similar to the length of the excimer resonator. The number of modes per unit volume per unit frequency which can exist in a cube is given by¹:

$$\rho(\nu) = \frac{8\pi\nu^2 n^3}{c^3}$$

where:

- $\rho(\nu)$ modes per unit vol. per unit freq.
- ν frequency
- n index of refraction
- c speed of light in vacuum

If we assume a cube with side length equal to the excimer's resonator length, l , then the total number of possible modes in the cube for a spectral linewidth of $\Delta\nu$ is:

$$N = \frac{8\pi\nu^2 n^3 l^3 \Delta\nu}{c^3}$$

where:

- N total number of modes in cube
- $\Delta\nu$ laser spectral linewidth
- l laser resonator length

This result, N , is the number of modes which could exist in a cubic resonator. The excimer's modes are a subset of this total which can exist in the long narrow volume of the excimer resonator. Taking the ratio of true resonator volume to cubic volume will give a good approximation of the actual number of modes in the excimer, call it N_r . The output mirror of the excimer is 17.5mm by 7mm, and, with a resonator length of one meter, defines the resonator volume. The number of modes in an unnarrowed excimer can be calculated using the following characteristics:

$$\begin{aligned}
 l &= 1 \text{ m} \\
 \text{resonator volume} &= 1.2\text{e-}4 \text{ m}^3 \\
 \nu &= 1.2\text{e}15 \text{ Hz (248 nm)} \\
 \Delta\nu &= 2.4\text{e}12 \text{ Hz (0.5 nm)} \\
 n &= 1
 \end{aligned}$$

Giving:

$$N_r = 3.9\text{e}14 \text{ modes}$$

The line narrowed excimer has a $\Delta\nu$ of $1.5\text{e}10$ Hz (0.003 nm) and possesses a possible $N_r = 2.3\text{e}12$ modes. The nonzero reflectivity of the front mirror helps to create a cavity which induces some mode competition and thus these calculations give the highest possible estimate for mode count. References have given values as low as $1\text{e}7$ modes for unnarrowed excimer lasers².

2.2. Profile Measurements

These crude estimates of mode count all lead to the conclusion that radiation from an excimer should not be diffraction-limited or spatially coherent. The excimer beam was measured with the two dimensional imaging system. The excimer beam is several times larger than the imaging array so some image reduction must be performed. The system used to accomplish this is shown in fig. 3.3. The 200mm focal length lens images the plane in front of the 1000mm lens onto the array with approximately 5:1 reduction. The 1000mm lens acts as a field lens so that every point in the object plane is presented with the same numerical aperture. The 200mm lens is operating at $\text{NA}=0.10$ so the geometrical aberrations introduced are minimal.

Fig. 3.4 shows the beam profile for the unnarrowed excimer laser. The flat top profile along the x-axis is evidence of the many transverse modes which exist in this direction. This flat top is well maintained from pulse to pulse and within each pulse. The approximate gaussian shape along the y-axis shows the reduction of mode count in this axis due to the more narrow exit window in the y direction. The correlation of this profile

with a true gaussian is 96 percent, so one can assume that modes other than TE_{00} exist but they carry much less energy than the fundamental.

Profiles of the line-narrowed laser, fig. 3.5, show an evident loss of uniformity. The flat top is now replaced by a large ripple and the well formed gaussian shape in the horizontal direction is lost. Integrating over many shots smooths the profile but does not produce a gaussian intensity in the horizontal direction. Fig. 3.6 is the sum of 32 pulses integrated onto the two dimensional measurement array. The random fluctuation in the beam profile is caused, in part, by changes in the refractive index of the lasing gas. The heavy inversion and hence high gain of the lasing gas leads to local changes in the refractive index. The unnarrowed excimer uses a greater lasing volume and does not have a wavelength-selective rear mirror. Because of these efficiencies, the unnarrowed laser is not pumped as hard, thus reducing the development of inhomogeneities.

3. Beam Divergence

It is of interest to note the specifications for beam size and beam divergence. Assuming that the beam waist is not too different than the beam size specified at one meter from the laser, one can calculate the diffraction limited divergence for such a beam size. It is not unreasonable to assume that the beam waist is the same as the beam profile at one meter since the true waist most likely occurs in the cavity and a divergence of 2 to 3mrad will not expand the beam significantly over one meter. The theoretical equation for diffraction limited divergence for a beam waist of ω_0 is given by:

$$\theta_{beam} = \arctan\left(\frac{\lambda}{\pi\omega_0 n}\right)$$

where n is the index of refraction and λ is the lasing wavelength. The diffraction limited divergence is 0.258mrad in the vertical direction and 0.646mrad in the horizontal. The excimer beam is thus 5 to 10 times more divergent than a diffraction limited beam of similar dimensions. This high divergence is another manifestation of the existence of

many modes in the beam as opposed to one or only a few as in most conventional laser systems.

The setup used to measure the beam divergence is shown in fig. 3.7. The 2-D array is placed at the focal plane of a 1000mm focal length lens. To find the focal plane, a well-collimated beam is input to the lens and the 2-D array is adjusted to attain smallest spot size. The raw laser is then input to the lens and array system. The resulting intensity profile gives the amount of energy emitted versus divergence angle. This result is shown in fig. 3.8. The divergence of the laser beam is defined as the angle with $1/e$ intensity. These measurements give a divergence of 1.91 mrad in one direction and 3.93 mrad in the other.

4. Spectral Linewidth

The major difference between the unnarrowed and line narrowed lasers is the wavelength-selective reflector in the rear of the line-narrowed laser. The addition of this element reduces the laser's linewidth from 0.5 nm to 0.0016 nm. The setup for measuring the linewidth is shown in fig. 3.9³. The apparatus consists of a Fabry-Perot interferometer, a diffuser plate, and beam delivery optics. The interferometer is constructed from two dielectric mirrors coated for maximum reflectance at normal incidence. The mirrors are $\lambda/10$ flat over their two-inch diameter. The interferometer uses only the center half inch of each mirror, so the useful mirror flatness is nominally $\lambda/40$. With a mirror spacing of 6 mm the interferometer has a free spectral range of 5.1 pm. The system has a practical resolution better than 0.5 pm. The diffuser plate is necessary to measure the radiation from all modes of the laser. Without the diffuser, the interferometer will select only a subset of the modes that exist in the output beam, leading to a measurement of a smaller linewidth than actually exists in the full output beam. An analogous situation exists in lithography equipment using excimer laser sources. If only a fraction of the available

modes are used, interference and speckle problems will be increased unnecessarily.

Fig. 3.10 shows the familiar bull's eye pattern at the focal plane of the output lens from the Fabry-Perot interferometer system. Each peak is separated by 5.1 pm and has a 1.6 pm width at half maximum. This measurement system gives no information about the absolute wavelength position of the output radiation, only the width of the line is obtained.

5. Coherence Length

A second method of verifying the output linewidth is to measure the coherence length of the laser. A Michelson interferometer shown in fig. 3.11 is used for this purpose. Fringes are created by the interference between the two beams generated with a beam-splitter. The fringe modulation is measured using the two dimensional CID detector array. A plot of fringe contrast versus path length difference is given in fig. 3.12. Fringe contrast is defined as:

$$C = \frac{I_{\max} - I_{\min}}{I_{\max} + I_{\min}}$$

A perfect contrast of one is not produced at zero path difference because of the imperfect flatness of the mirrors and the unequal losses through the two paths. We assume the line shape to be gaussian and performed curve fitting on the data. The best fit was obtained for a spectral linewidth of 1.6 pm. The coherence length defined by:

$$\Delta l = \frac{\lambda^2}{\Delta \lambda}$$

is 38 mm for this spectral width. The etalon measurement and Michelson measurement of spectral linewidth agree well within experimental error.

6. References

1. A. Yariv, *Quantum Electronics 2nd Edition* John Wiley and Sons, New York, pp. 95-97, 1975.
2. H. Pummer, "The Excimer Laser: 10 Years of Fast Growth," *Photonics Spectra*, May 1985.
3. B. Ruckle, et. al., *Computerized Wavelength Stabilized 248.4 Excimer Laser for Microlithography*, Proc. of SPIE on Microlithography, Vol. 922, pp. 450-453, Mar. 1988.

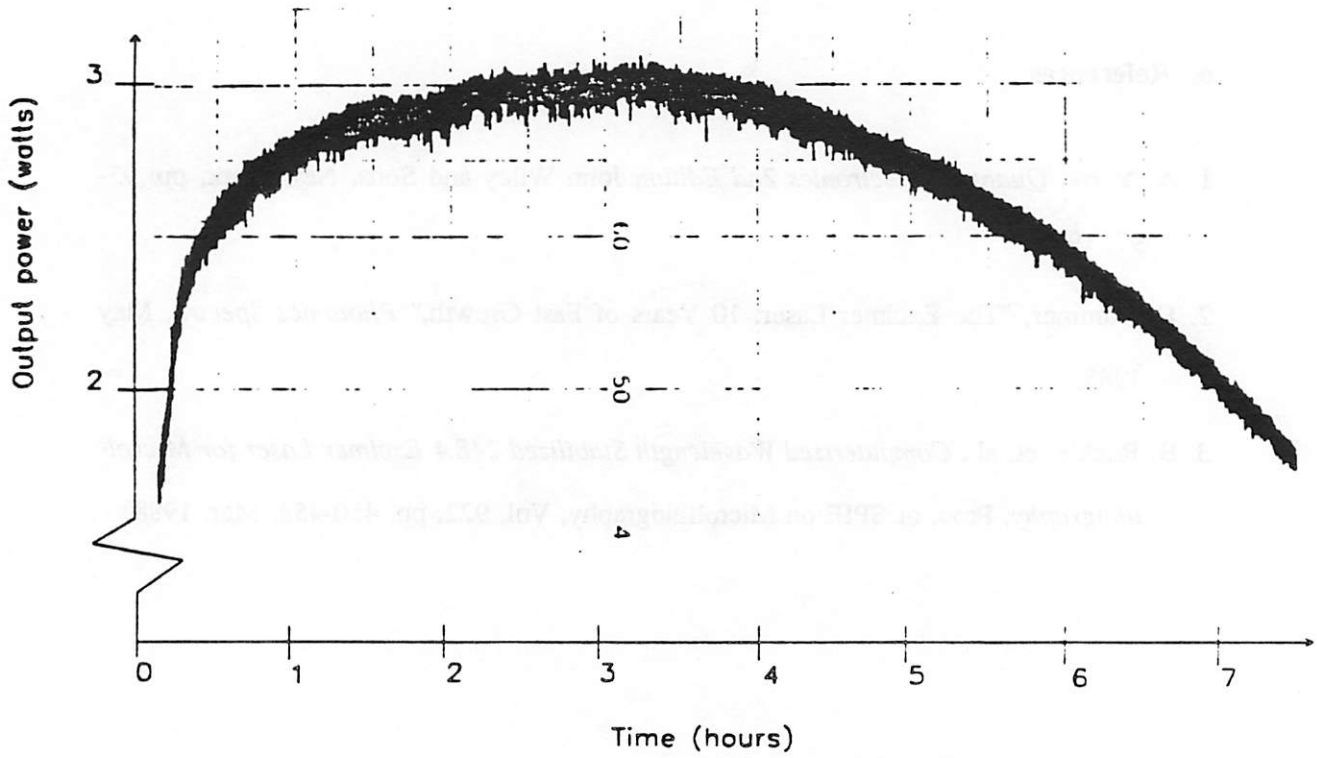


Fig. 3.1 Average power vs. time for fixed electrode voltage.

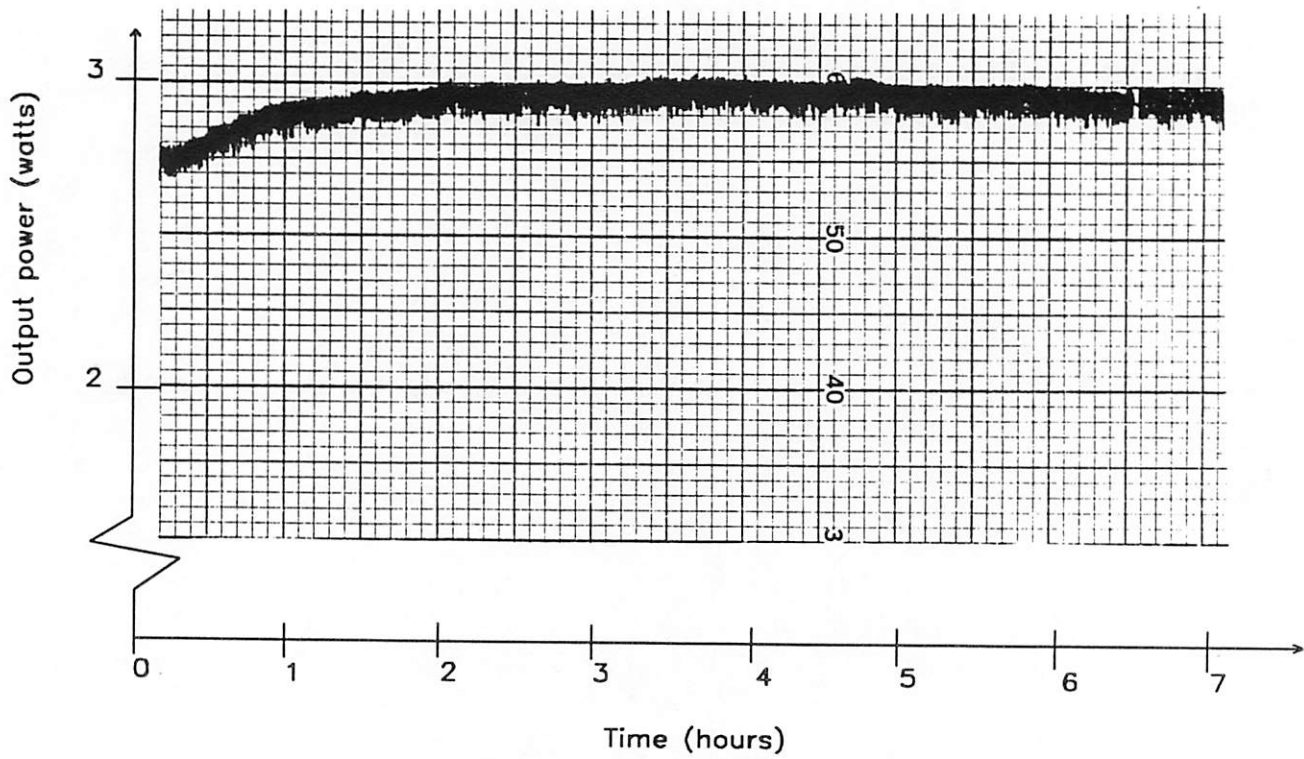


Fig. 3.2 Average power vs. time for constant output energy.

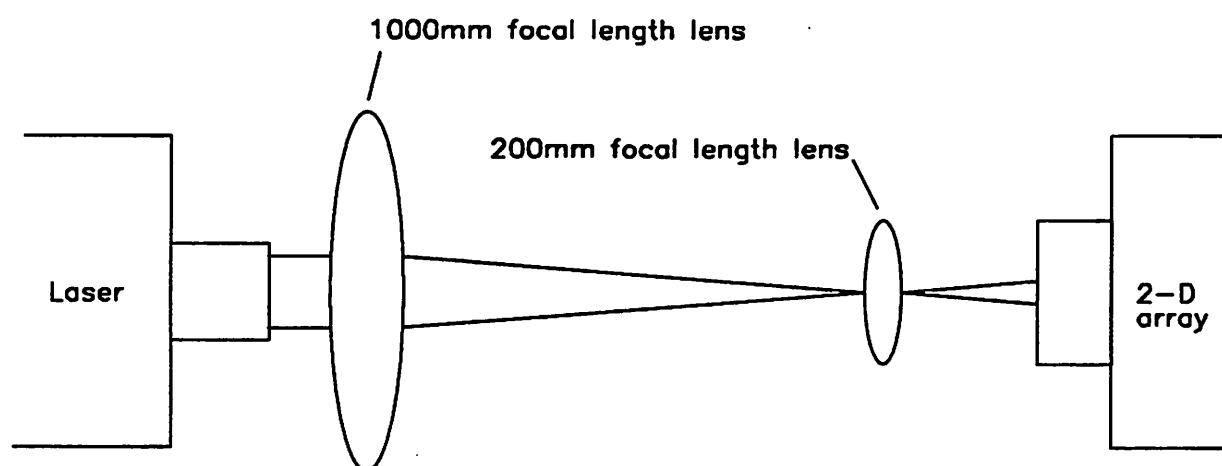


Fig. 3.3 Apparatus to measure beam profile.

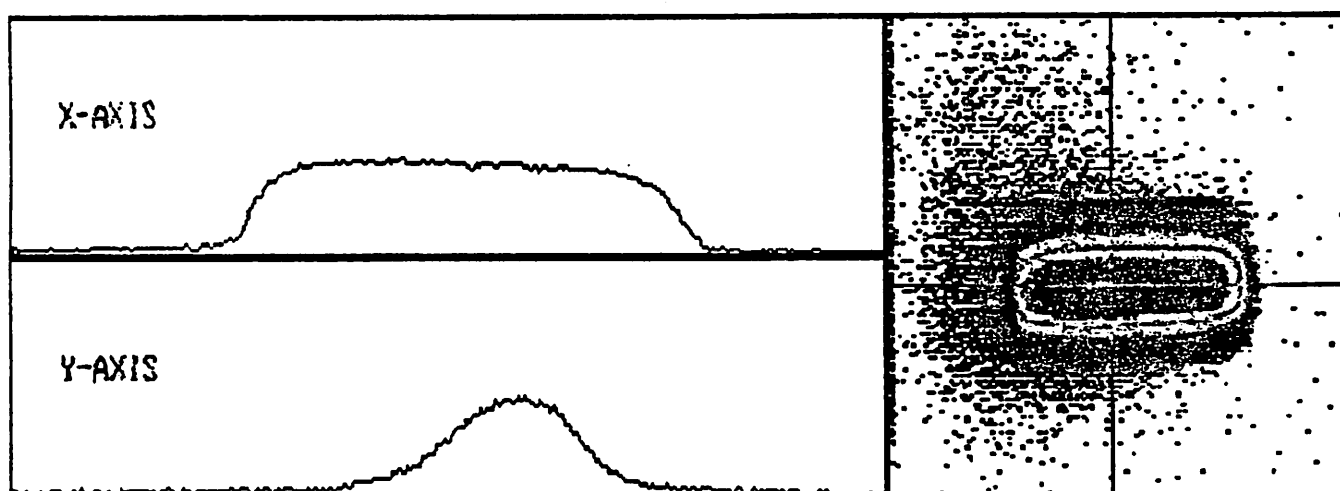


Fig. 3.4 Beam profile for unnarrowed excimer laser (single shot).

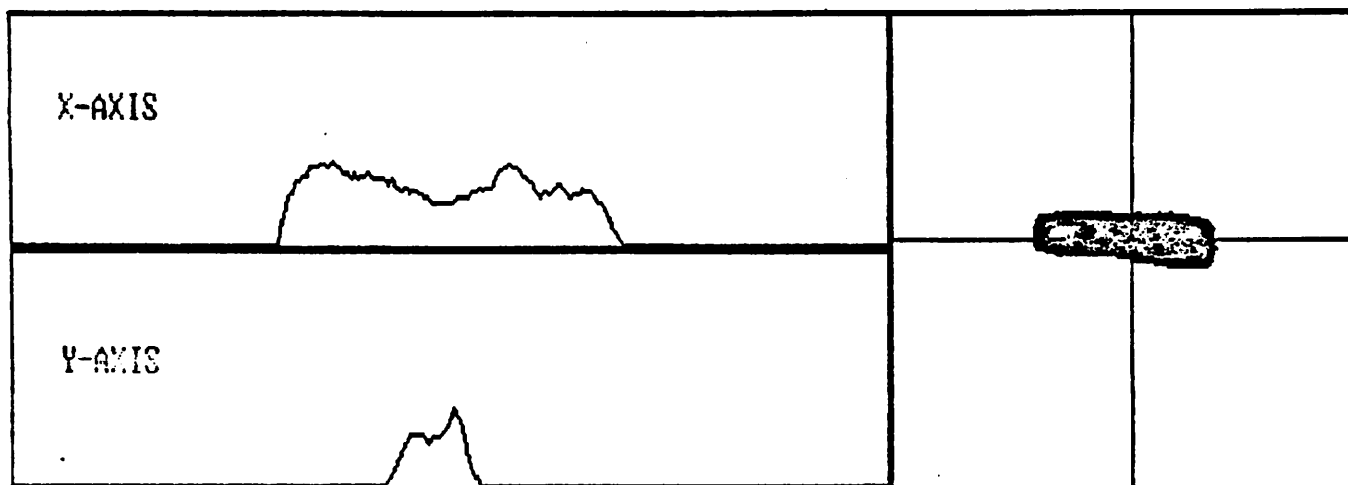


Fig. 3.5 Beam profile for line-narrowed excimer (single shot).

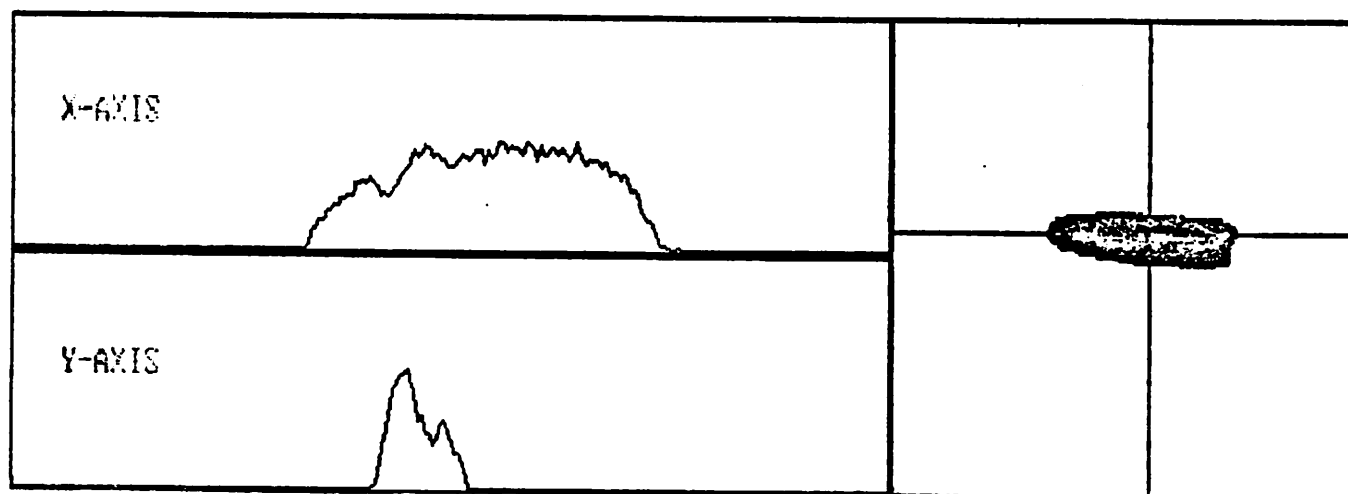


Fig. 3.6 Beam profile for line-narrowed excimer (32 pulses).

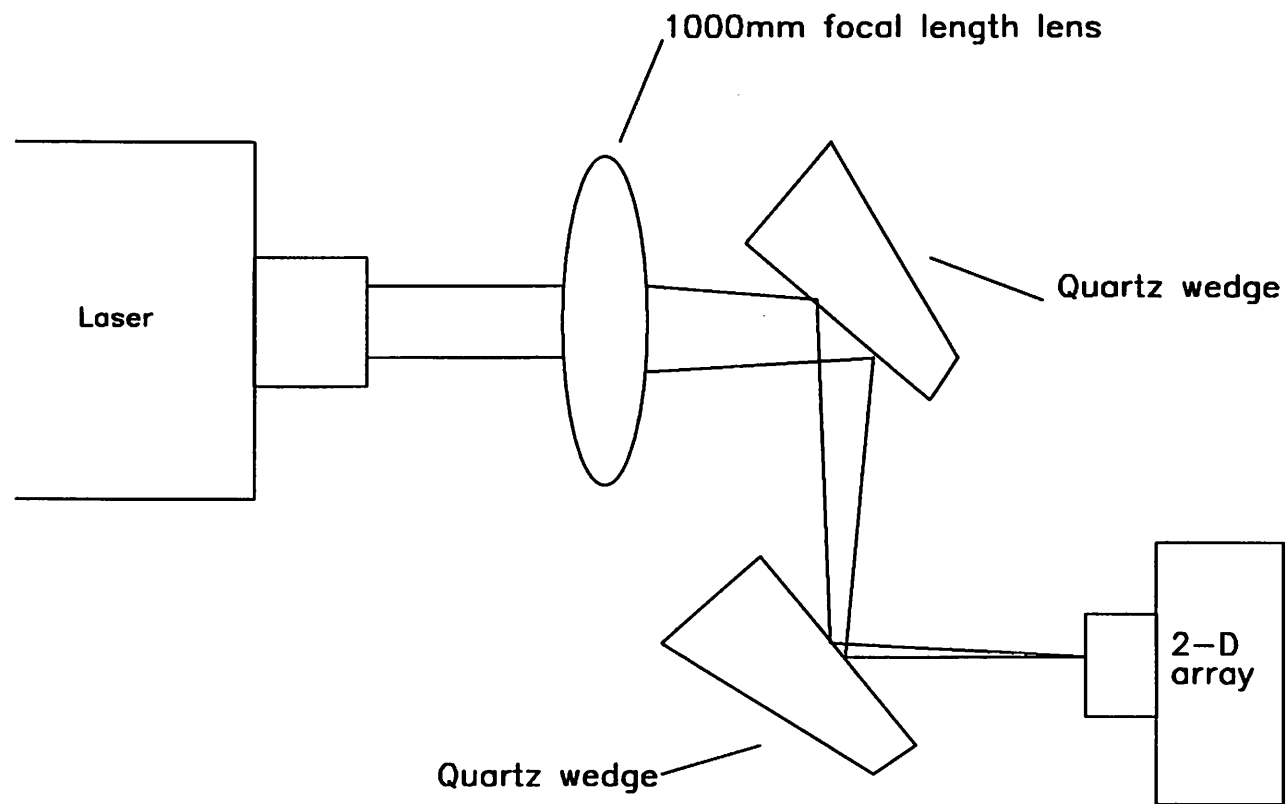


Fig. 3.7 Apparatus to measure beam divergence.

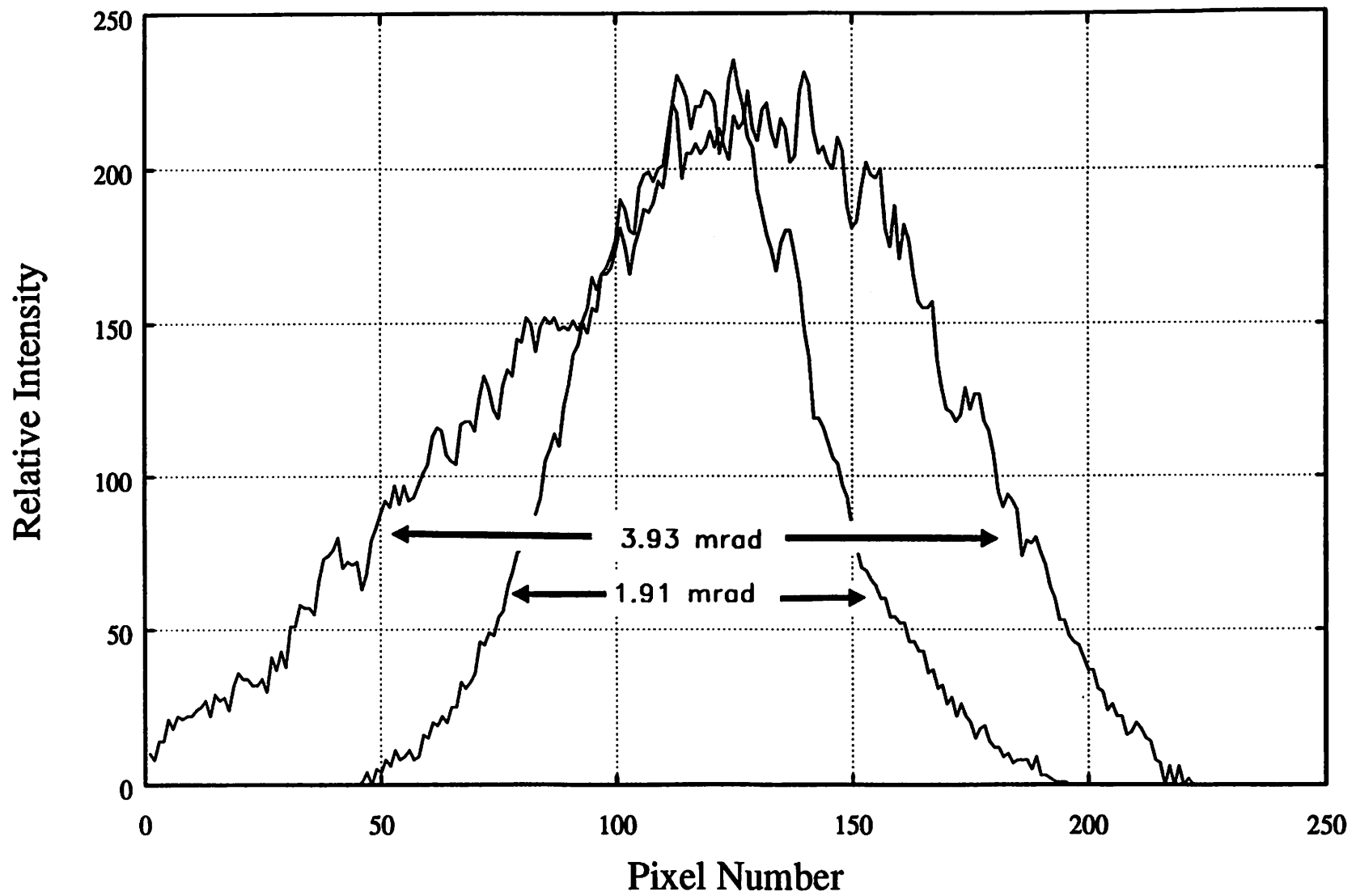


Fig. 3.8 Relative intensity vs. divergence angle.

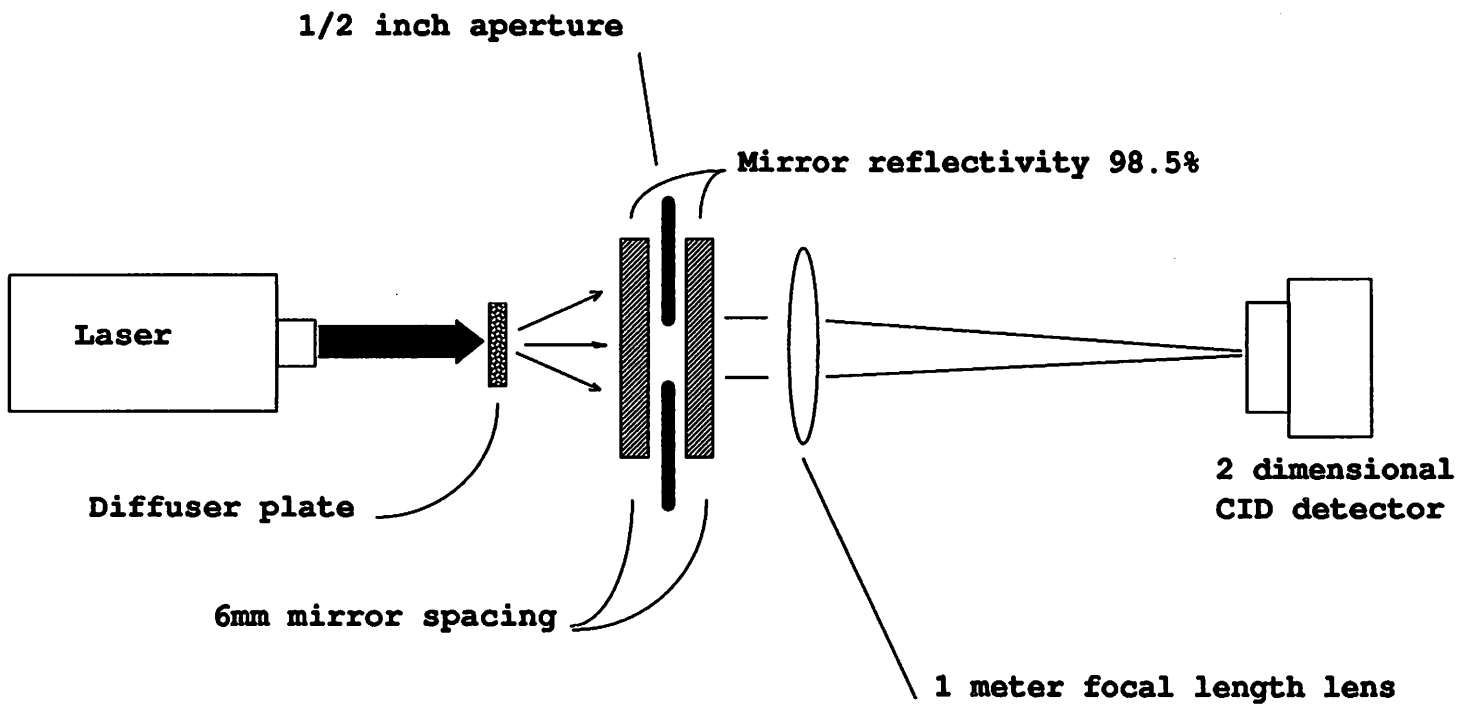


Fig. 3.9 Apparatus for measuring laser spectral linewidth.

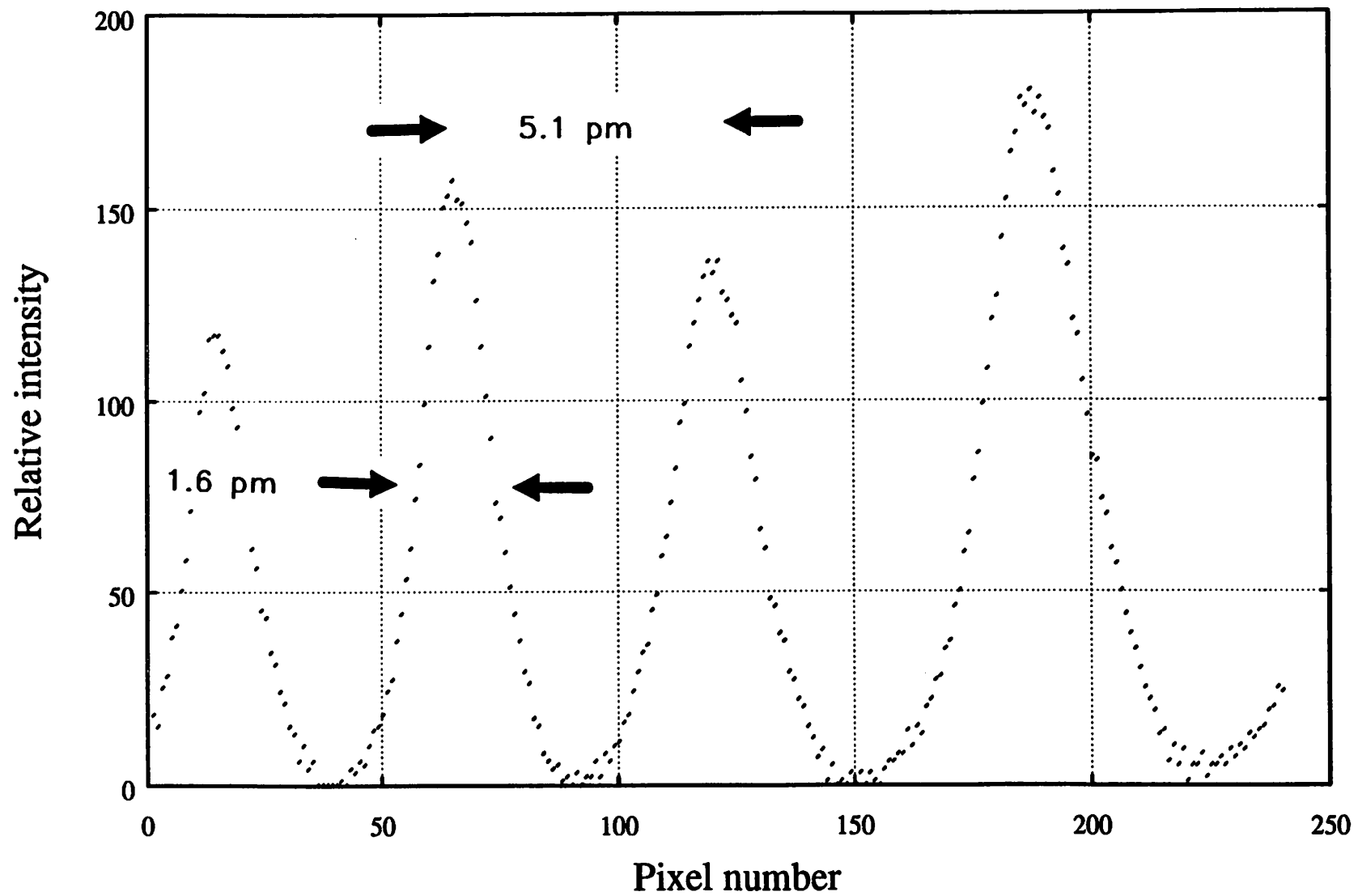


Fig. 3.10 Bull's Eye pattern from Fabry-Perot etalon.

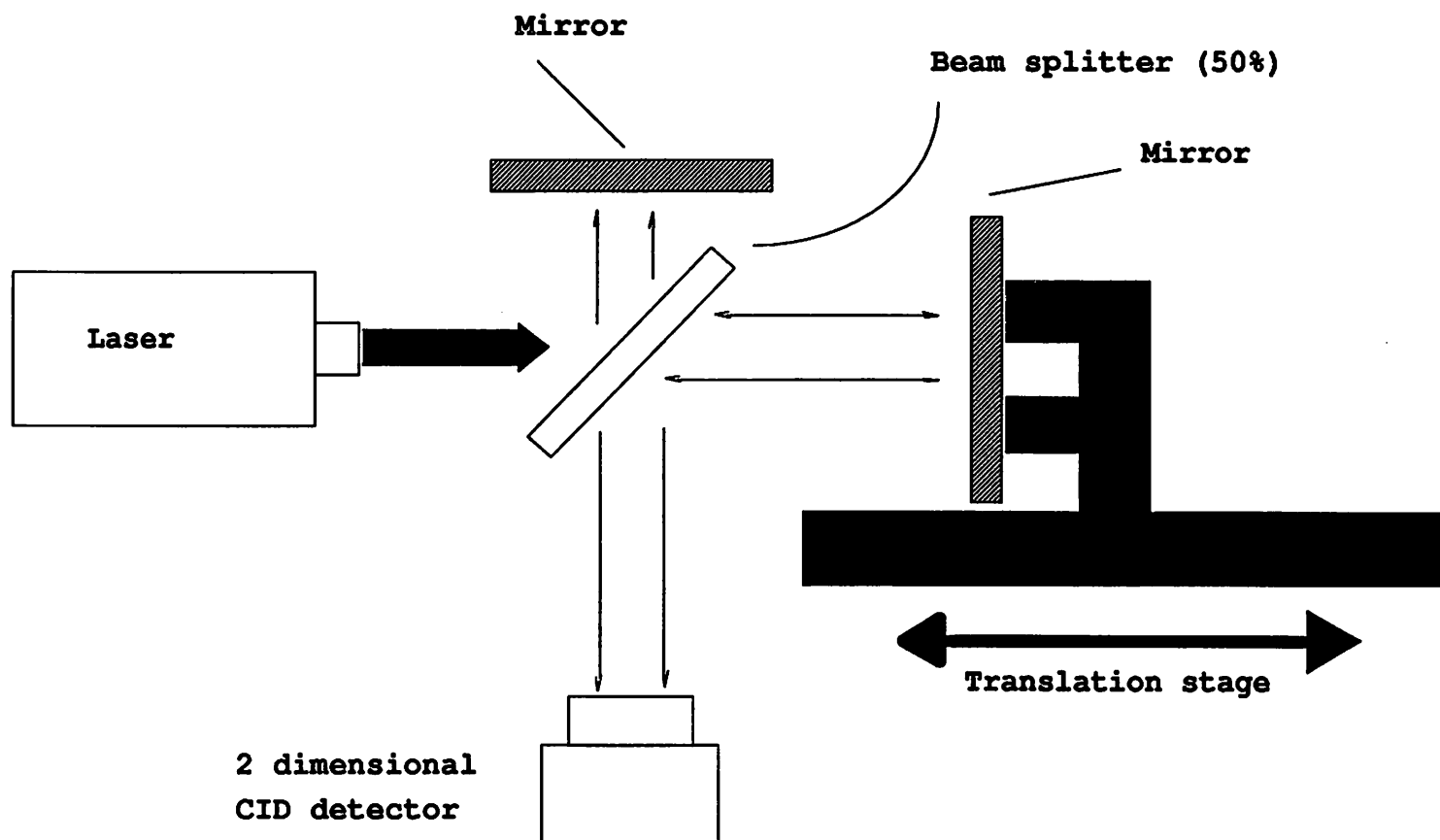


Fig. 3.11 Apparatus for measuring laser's coherence length.

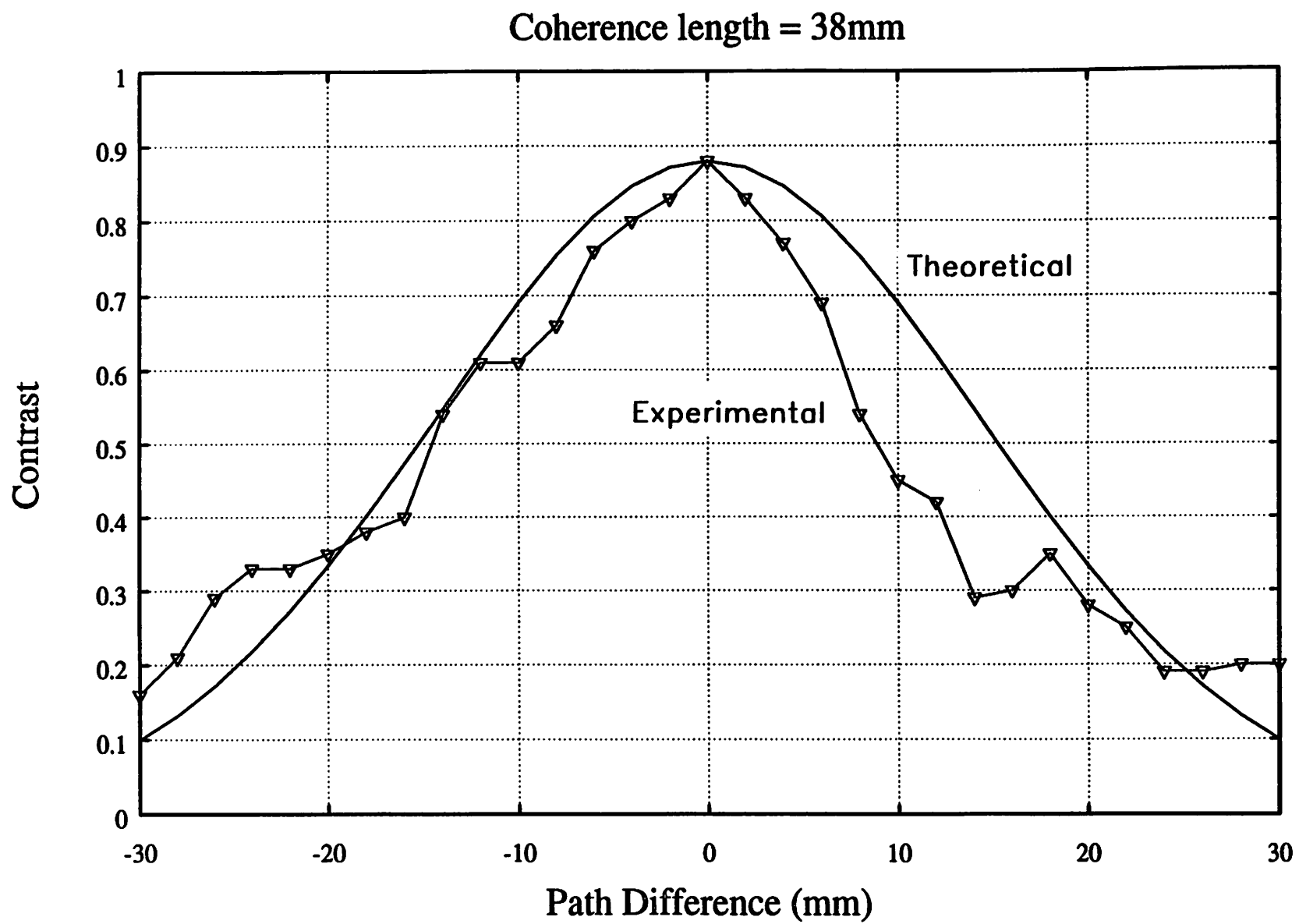


Fig. 3.12 Fringe contrast vs. path length difference.

Chapter 4: Illuminator Components

1. Square Light Pipe

A 38 mm coherence length represents a challenging problem in optical design. Any component which separates the laser beam into parts which travel different paths before they recombine has the potential for creating unwanted fringes. Light pipes and diffuser plates do just this.

Light pipes produce a uniform illumination while increasing the source size as seen by the illuminating optics.^{1 2} To feed the light pipe, one needs to produce a spread of rays from the essentially parallel ray laser beam. A short focal length lens or a diffuser plate can be used. This cone of rays is folded back onto itself several times, producing many virtual sources at the input plane. Fig. 4.1 shows the ray bundle folding and the virtual sources created.

These virtual sources all illuminate the exit plane of the light pipe. Each source individually may be nonuniform but the sum of many such sources becomes uniform. The more sources produced the greater degree of uniformity at the exit plane. To increase the number of sources produced, the light pipe could be lengthened or the input cone angle could be increased. The extent of the input cone angle controls the size of the exit cone angle from the light pipe. Considerations of the condenser system and lithography lens will determine the required exit cone angle from the light pipe, and thus prescribe the input cone angle.

Two conditions limit the length of the light pipe. The first is simple physical size. The second is the path difference between each virtual source produced by the light pipe. Short wide light pipes introduce a larger path difference between adjacent sources than do long narrow light pipes. With the limited coherence length of an unnarrowed excimer laser, this path length difference helped suppress fringe formation. However, with the 38

mm coherence length of the line narrowed excimer, creating sources with path separations greater than the coherence length becomes impractical.

The light pipe used in the U.C. Berkeley large area exposure system is a square, air filled light pipe constructed from four pieces of glass glued at right angles and coated with aluminum. It is 5 inches long and one half inch on each side. The Berkeley light pipe can be illuminated with either a lens or a diffuser plate. The lens gives greater system efficiency while the diffuser plate produces more uniform illumination. Since the path differences between the virtual sources are much less than the coherence length, fringe patterns are created at the exit plane of the light pipe. The exit plane of the light pipe is imaged onto the mask and thus fringes also exist at the mask plane (fig. 4.2). Fig. 4.3 is a microphotograph of the illumination produced by the light pipe when illuminated with a lens. One can see the fringe pattern characteristic of a square light pipe. Fringes are created at right angles to each other because the virtual sources produced by the light pipe are in a regular square pattern.

Use of the diffuser plate in place of the lens gives less fringe modulation at the exit plane of the light pipe. This can be shown by drawing an analog between the light pipe and Young's experiment. Young's experiment consists of two sources interfering at a plane some distance away. Only a single source is needed if one uses Lloyd's mirror as shown in fig. 4.4. The second source is simply the grazing incidence reflection of the single real source. In this experiment the fringe visibility varies as the $\sin x/x$ of the source size.³ This theory describes the reduction of fringe contrast for sources which are totally incoherent over their area. The excimer beam has some spatial coherence across its profile, but it is not totally coherent, so we would expect the trend of the theory to hold. In our light pipe we have essentially four Lloyd's mirrors, each creating secondary sources which interfere. The visibility of these fringes is reduced when the source size is increased. Using the lens as the input to the light pipe gives a small point source, using

the diffuser plate gives a larger extended source. Thus, the diffuser plate produces a lower fringe contrast.

2. Hexagonal Light Pipe

We have also examined the uniformity of a prototype stepper using a line-narrowed KrF excimer source, and a hexagonal light-pipe illuminator. Such a geometry will produce interference fringes at 60 degree angles. Fig. 4.5 is a microphotograph of a clear area imaged in negative resist. The dose given was set so that the resist was exposed through its transition region. This way we could see small differences in exposure values. The modulation shown here, though impossible to quantify, is only a few percent. While the effect is interesting, it is apparently so small that there is no effect on linewidth control.

3. Bold Illuminator System

The BOLD illuminator system consists of a diffuser plate and two simple lenses which image the diffuser plate into the entrance pupil of the BOLD lithography lens. The illuminator is designed for Kohler illumination. That is, each point on the diffuser plate contributes to every point at the mask plane. In this way a uniform illumination is achieved in spite of any nonuniformities in the radiation from the diffuser. Figure 4.6 is a schematic of the BOLD illuminator.⁴

The draw back of this system is the creation of speckle by the diffuser plate. The characteristics of this speckle are affected by the grain size of the diffuser, the magnification ratio of the illuminator lenses, and the coherence properties of the laser. The first two attributes of the illuminator system are fixed by the BOLD system design criteria. Of the coherence properties of the laser, only the spatial coherence can be varied to any substantial degree. The laser beam's spatial coherence has a dramatic effect on the uniformity of illumination at the mask plane.

Fig. 4.7 shows the system used to adjust the spatial coherence of the input beam. It is difficult to quantify the level of spatial coherence. In this case, the fraction of the total beam used for illumination will be a measure of the spatial coherence. The greater the magnification produced by the system shown in fig. 4.7, the greater will be the spatial coherence of the illuminating beam.

Two situations are shown in figs. 4.8 and 4.9. The raw excimer beam is input to the BOLD illuminator with its aperture stop wide open in fig. 4.8 and closed down to 3 mm in fig. 4.9. One can see the increased speckle noise created when only a small portion of the diffuser is illuminated (fig. 4.9).

The uniformity produced by the bold illuminator is also degraded by increasing the spatial coherence of the input laser beam. Figs. 4.10 and 4.11 show the noise produced by an input beam with a high degree of spatial coherence. The aperture stop is wide open for fig. 4.10 and closed down to 3 mm for fig. 4.11.

Fig. 4.12 is a graph of the RMS noise produced at the mask plane by the BOLD system when illuminated by various fractions of the total excimer beam. As the fraction of the total beam used decreases, the amount of spatial coherence across the diffuser plate increases. Two conditions are shown, the lower for the aperture stop wide open (17 mm) and the upper for the aperture stop 3 mm wide.

All the figures 4.8 through 4.11 are 96 shots integrated onto the imaging array. Comparisons of these noise levels with those from single shots show little difference. This fact demonstrates the minimal increase in uniformity gained by exposing with many shots. To help correct this problem, the diffuser plate was mounted on the motor and rotated during exposure. This result is shown in fig. 4.13. The input laser beam has high spatial coherence and the aperture stop is wide open, same conditions as fig. 4.10. The nonuniformity seen in the stationary system all but disappears when the diffuser plate is

rotated during exposure.

The drawbacks of a rotating diffuser system are the impossibility of single shot exposures and the vibrations introduced into the system by the rotating motor. Since the laser pulse lasts for only 30 ns, the diffuser is essentially frozen during a single pulse. The movement of the diffuser in between pulses accounts for the averaging which occurs for multiple pulses.

4. References

1. J.S. Wilczynski, *Optical Lithographic Tools, Current Status and Future Potential*, J. Vac. Sci. Technol. B 5(1), pp. 288-292, 1987.
2. B. Fan, R.E. Tibbetts, J.S. Wilczynski, and D.F. Witman, Pat. No. 4,744,615, Jan. 1986.
3. M. Born, and E. Wolf, *Principles of Optics*, pp. 256-268, Pergamon Press, 1986.
4. J.H. Bruning, W.G. Oldham, *A Compact Optical Imaging System for Resist Process and Lithography Research*, Proc. of SPIE on Optical/Laser Microlithography, Vol. 922, pp. 471-475, Mar. 1988.

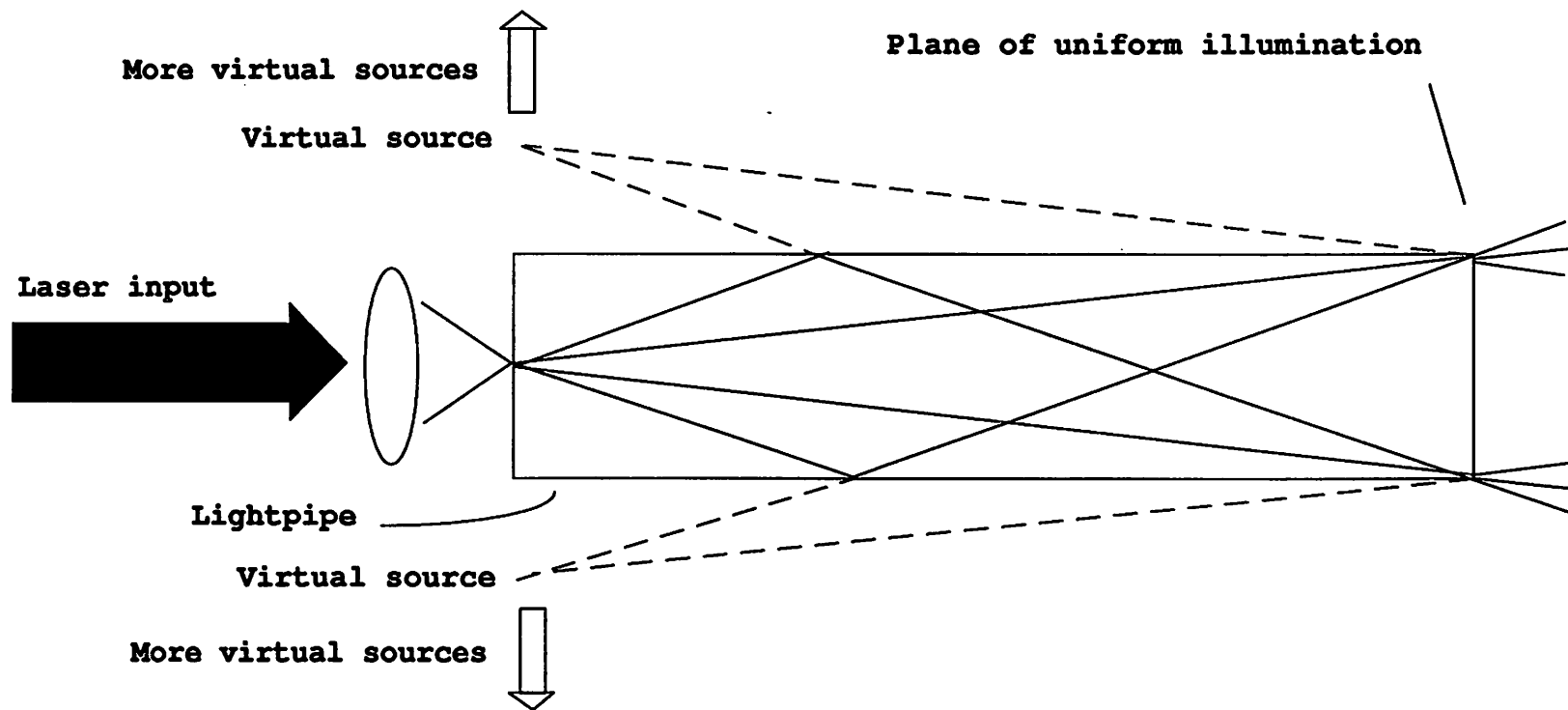


Fig. 4.1 Virtual sources and plane of uniform illumination created by light pipe.

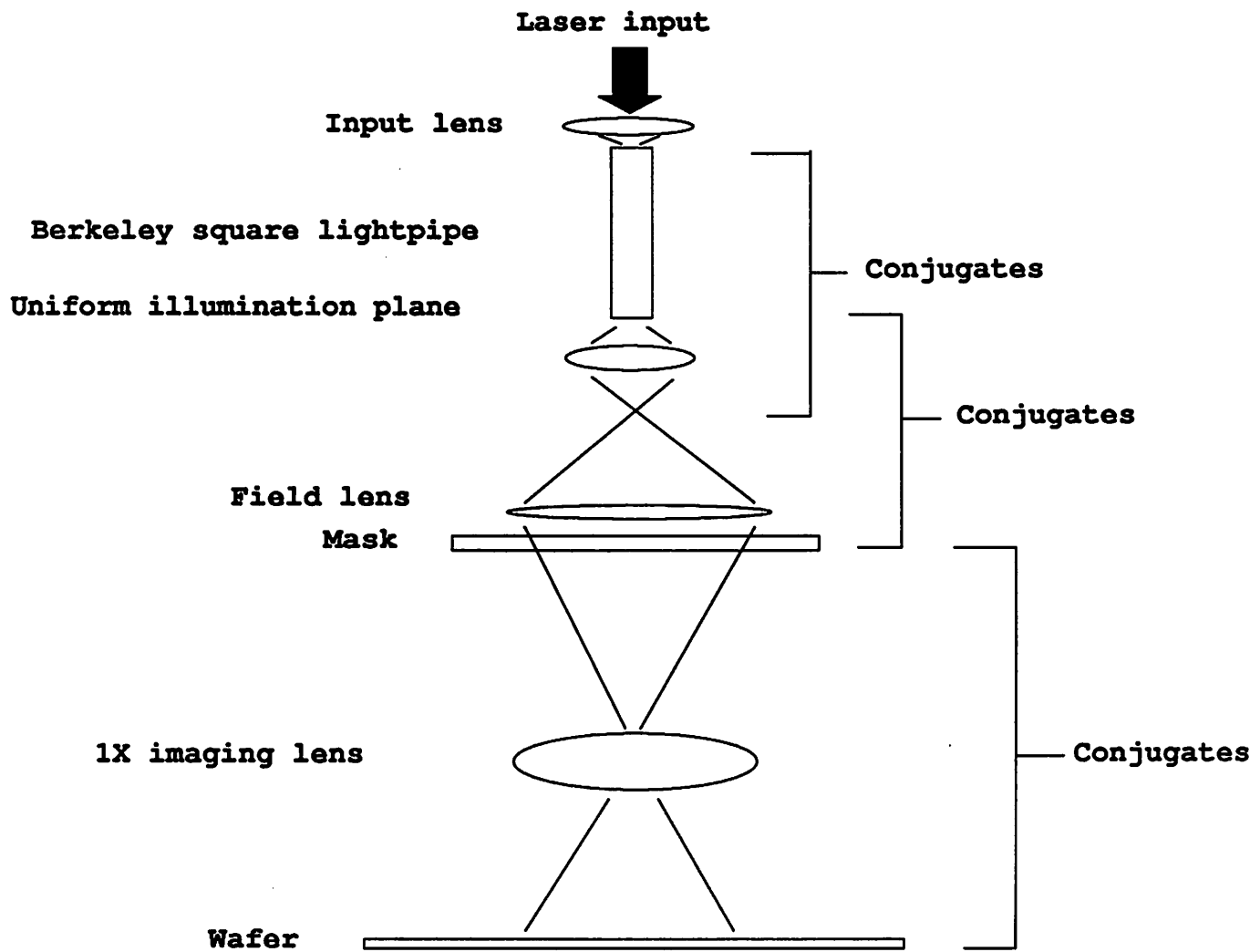


Fig. 4.2 Berkeley large area exposure system.

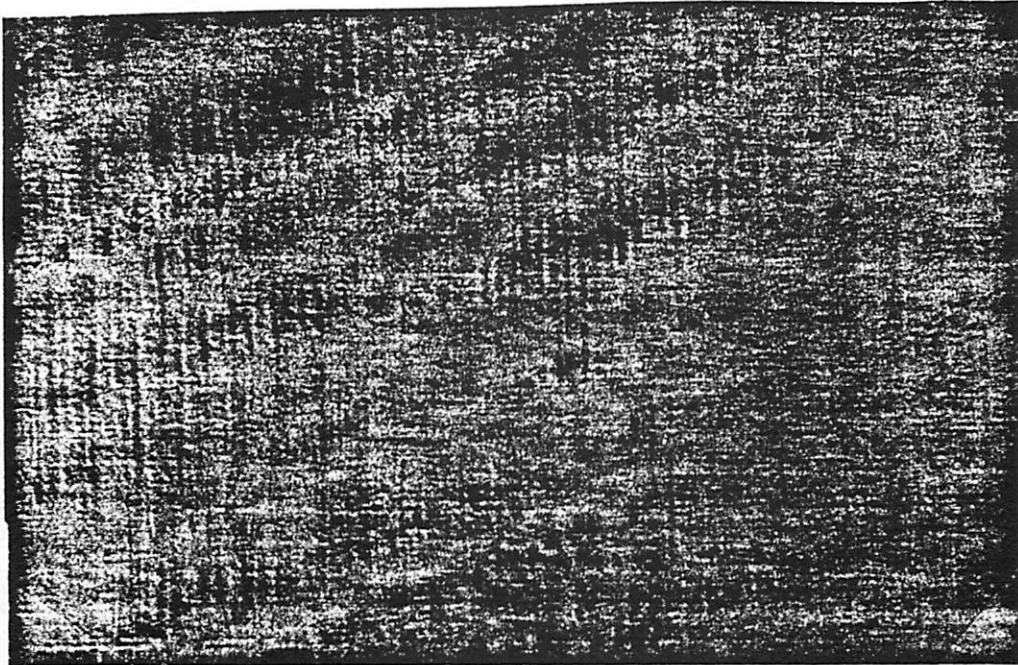


Fig. 4.3 Right angle fringes created by square light pipe.

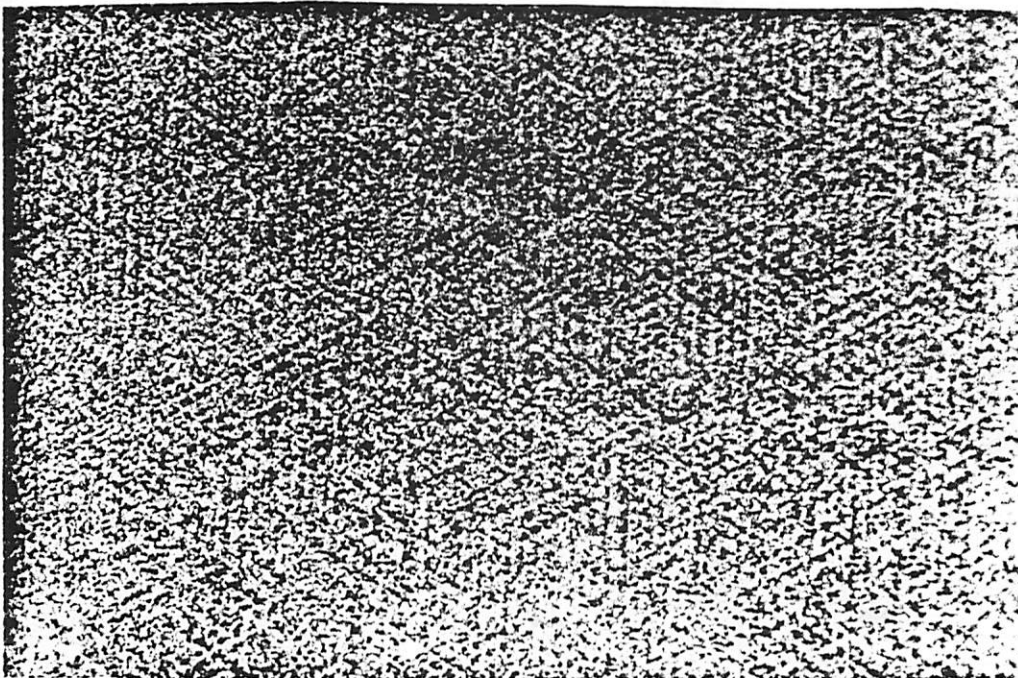


Fig. 4.4 60 degree fringes created by GCA hexagonal light pipe.

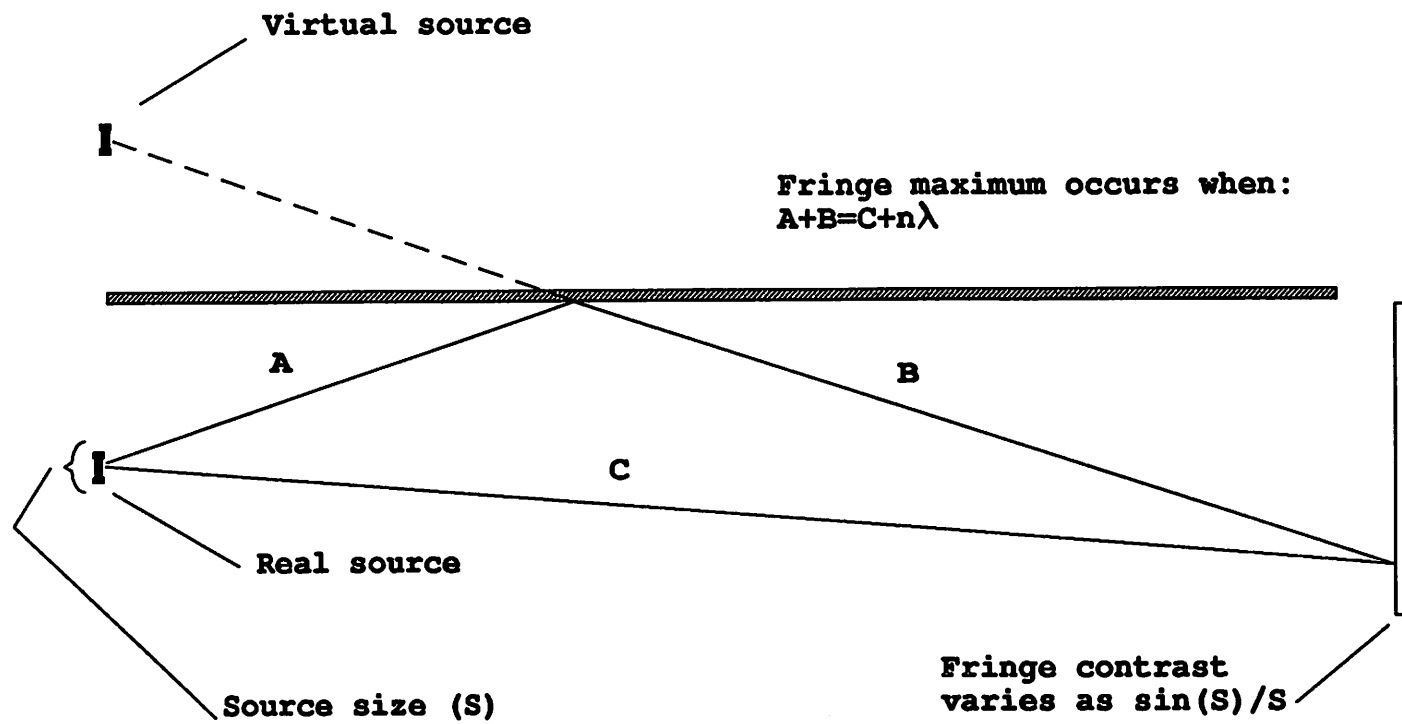


Fig. 4.5 Lloyd's mirror and fringe contrast vs. source size.

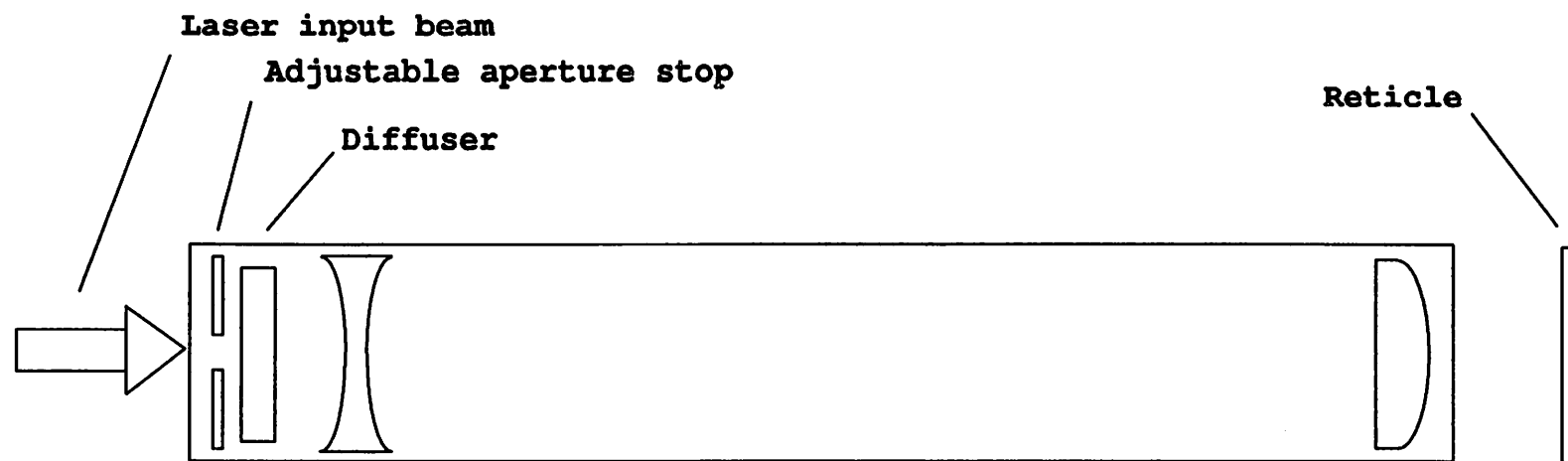


Fig. 4.6 BOLD illuminator system.

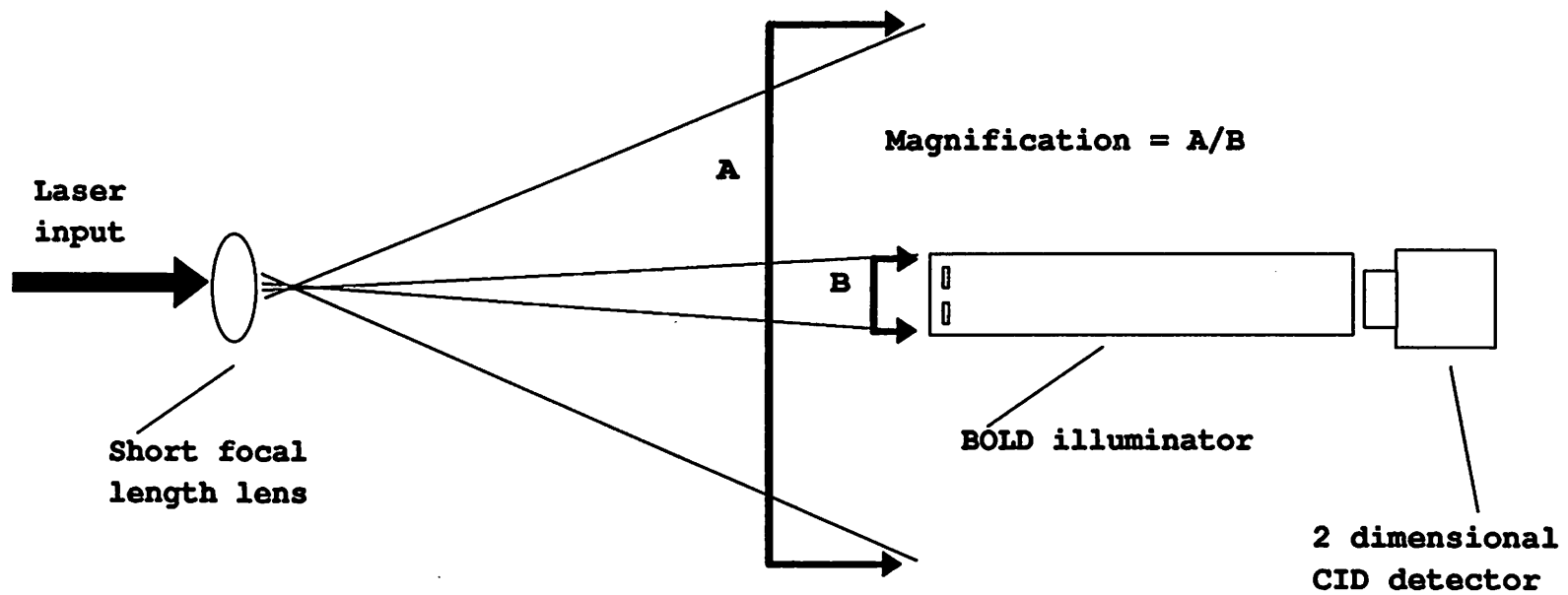


Fig. 4.7 System used to vary spatial coherence of illuminating beam.

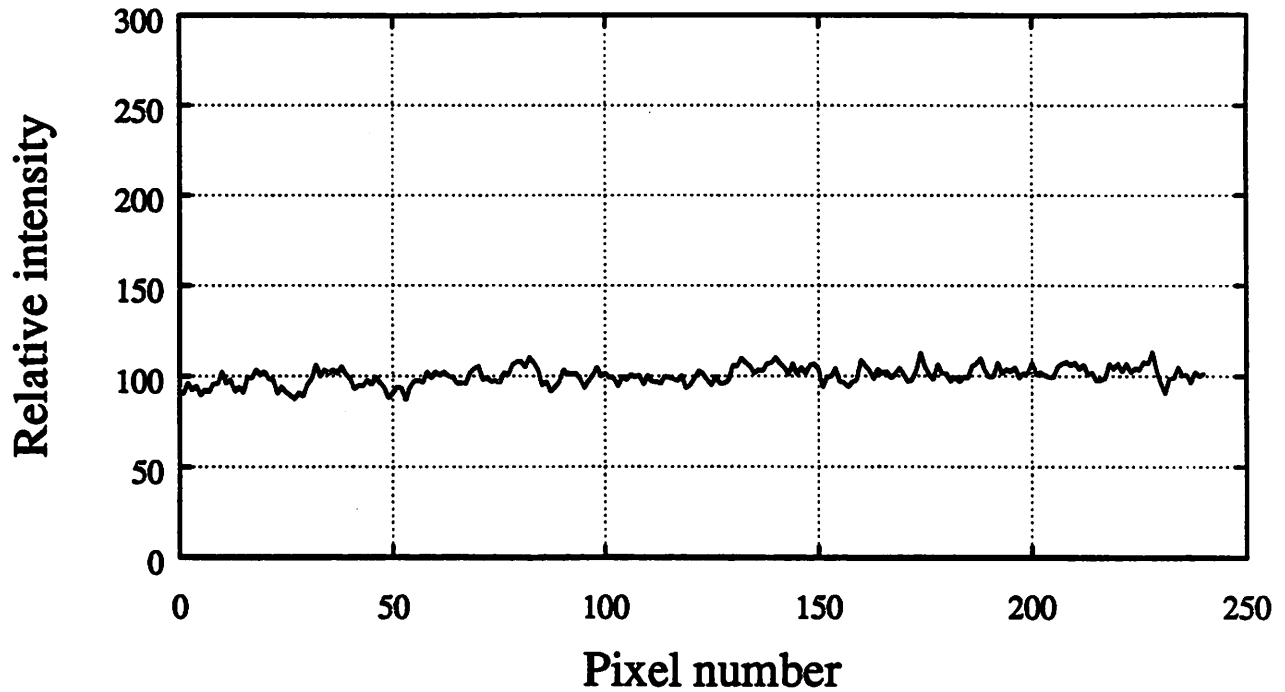


Fig. 4.8 Illumination uniformity produced with raw laser input and aperture stop wide open (17 mm).

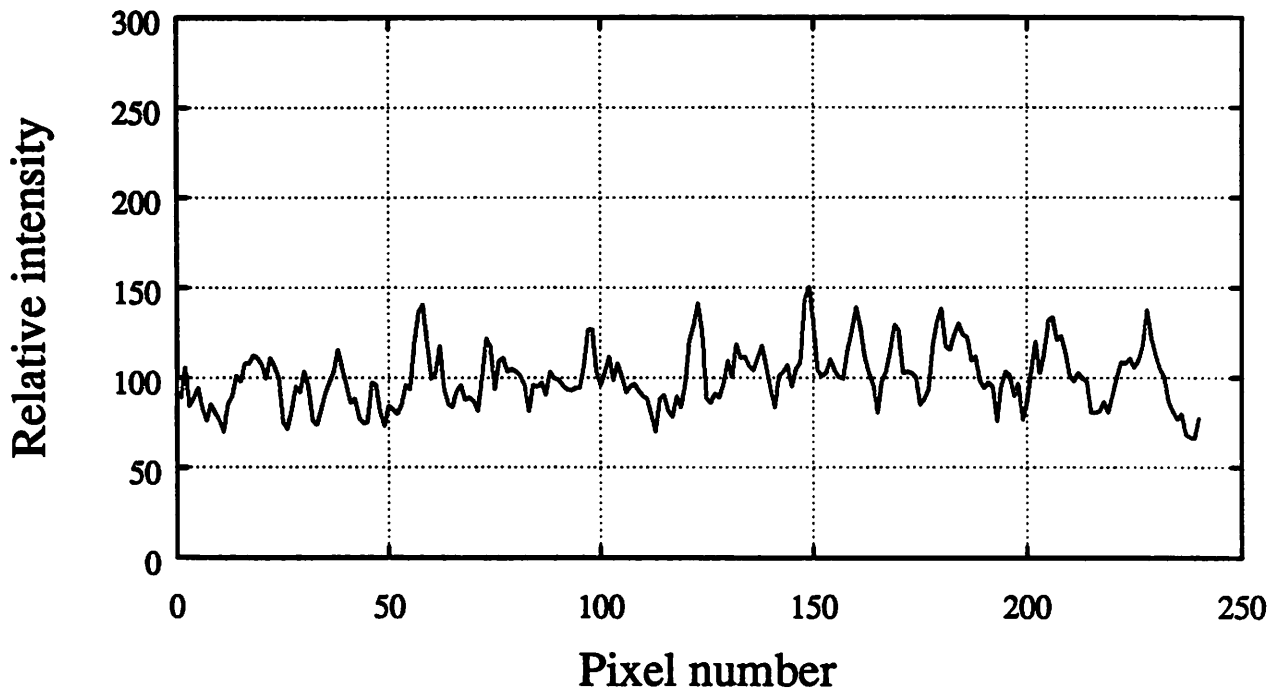


Fig. 4.9 Illumination uniformity produced with raw laser input and aperture stop 3 mm wide.

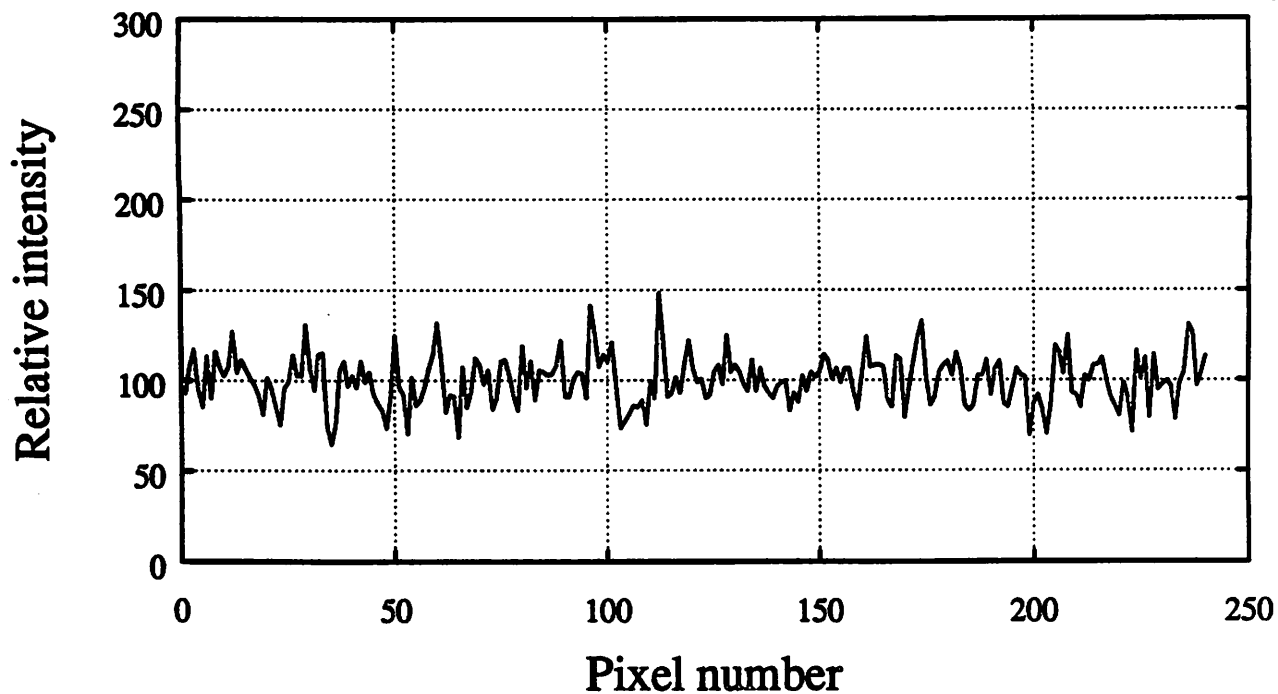


Fig. 4.10 Illumination uniformity produced with high spatial coherent input beam and aperture stop wide open.

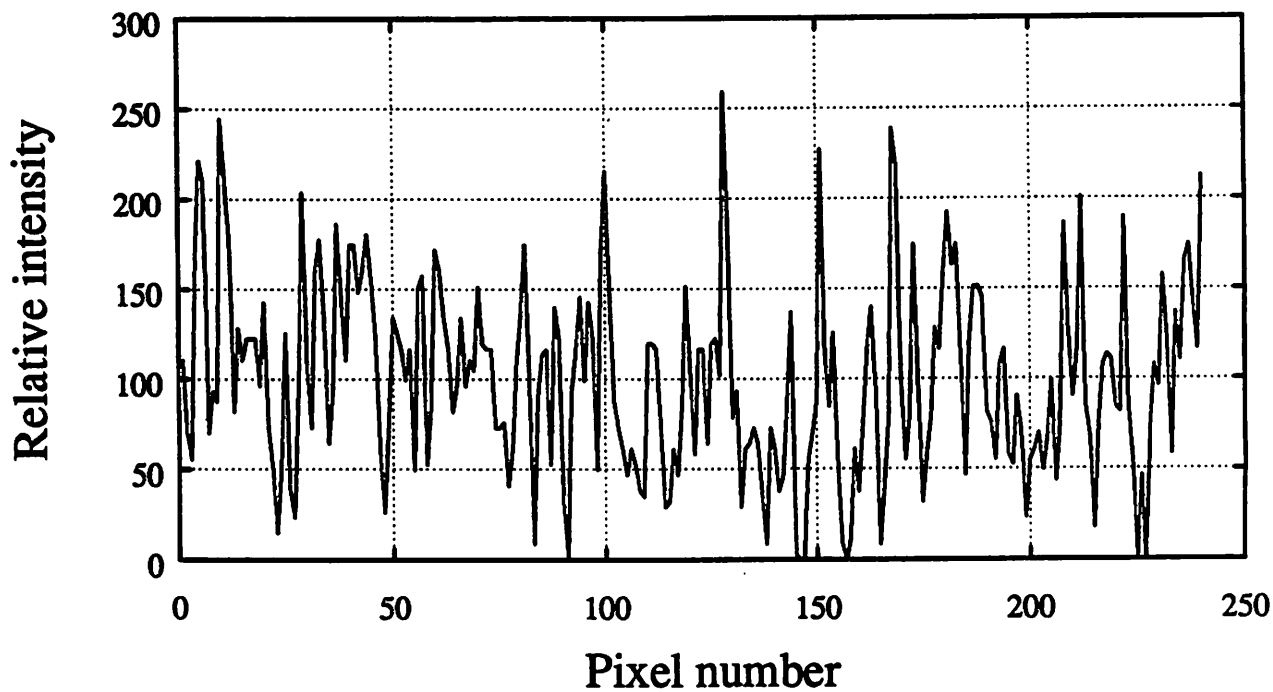


Fig. 4.11 Illumination uniformity produced with high spatial coherent input beam and aperture stop 3 mm wide.

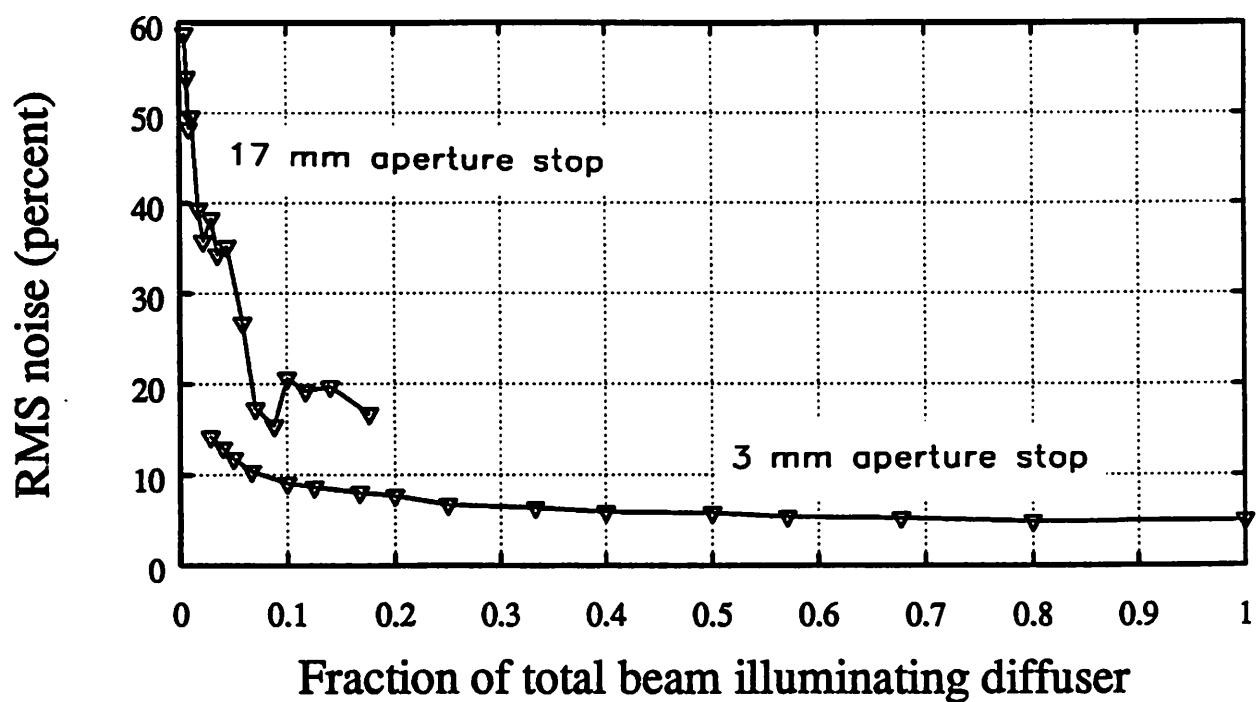


Fig. 4.12 Noise at the mask plane of the BOLD illuminator vs. fraction of total excimer beam input.

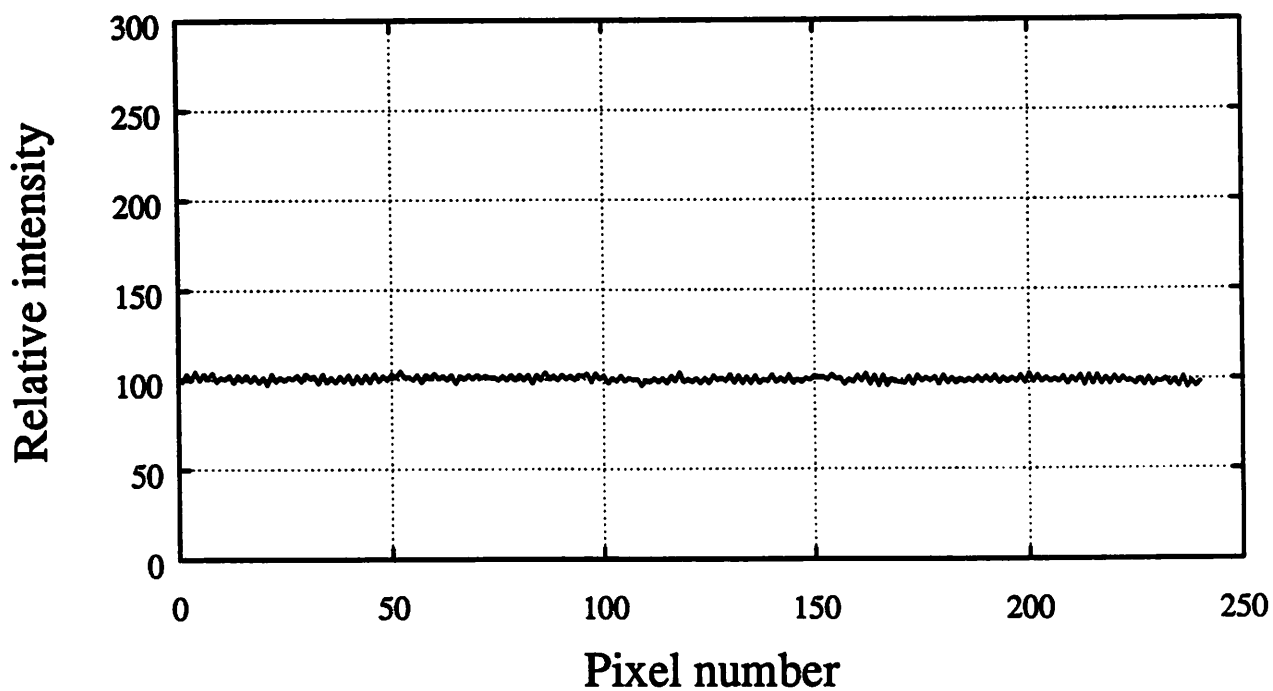


Fig. 4.13 Illumination uniformity produced with rotating diffuser plate.

Chapter 5: Conclusion

This report has shown that the radiation properties of excimer lasers can have a detrimental effect of illuminator systems for microlithography. The line-narrowed excimer laser's relatively long coherence length leads to fringe formation in any system which produces multiple paths to the illumination plane. This fringing can be kept to a minimum by taking advantage of the poor spatial coherence of the excimer's radiation. Collecting the maximum number of rays from the laser and using them throughout the illuminator system helps to reduce the modulation level of any fringes created by an illuminator system. Using the full excimer beam can be thought of as using multiple laser sources, since the beam is incoherent between points well separated across the beam profile.

Finally, after all techniques for reducing fringe contrast in a single laser pulse are exhausted, one can employ moving components within the illuminator system. This will not reduce the fringe formation within a single pulse but will change the fringe pattern from pulse to pulse. Averaging over many pulses will then give the net result of uniform exposure.

Appendix A: Laser Gas Change Details

Refer to fig. 2.2 in the text. A typical gas change procedure is as follows. First start the vacuum pump and open V6. Wait until the gauge G1 reads below 500 mtorr, then open the bypass valve V5. When the vacuum gauge falls again below 500 mtorr, all the major tubing will then be evacuated, close V6. Open the cylinder valve on the helium take. The helium regulator should be set to a bit over atmospheric pressure. Crack V1 until the pressure on gauge G2 reads 780 torr, close V1. Open V6 until G1 reads below 200 mtorr, close V6. Repeat the last two steps again, the supply plumbing will then be purged and clean.

Now, with V1 and V6 closed, close V5. Open the outlet valve and the laser, then open V7. The excess pressure in the laser will now bleed through V7 through the Fluorine trap into the microlab exhaust system. After a few minutes the excess pressure will be relieved, close V7. Open V6, this will pump out the remaining gas from the laser. When G1 falls below 200 mtorr close V6 and the laser outlet valve. Now open the laser inlet valve and crack V1 until G1 reads 780 torr. Close V1 and the laser inlet valve. Shut off the helium cylinder valve. The laser is now filled with one atmosphere of helium.

Open V6 then open the laser outlet valve. When G1 falls below 200 mtorr, close the laser outlet valve. Now, open V5 and wait until G1 again reads below 200 mtorr, close V6 and V5. Turn off the vacuum pump. Finally, open the laser inlet valve and open the KrF cylinder valve. The KrF regulator should be set a bit above 2600 torr. Crack V2 until G2 reads 2600 torr. There will be some time delay in the G2 reading, so approach the 2600 torr level slowly. When G2 reads 2600 torr, close V2, the KrF cylinder valve, and the laser input valve.

The last step is to enter the two cylinder pressure readings in the microlab computer

under the equipment heading "excimer" or "X" for short.

Appendix B: Camera and Laser Synchronization

1. Single Shot Synchronization

Refer to fig. 2.4 in the text. The camera system provides and expects synchronization signals when imaging pulsed light sources. The camera sends a TRIG OUT signal to the laser signifying that the camera is ready for a laser pulse. This TRIG OUT signal is derived from the vertical sync signal of the camera. A TRIG IN signal is needed from the laser within 500 μ s of the TRIG OUT signal for the system to consider the pulse valid. When the laser receives the TRIG OUT signal it holds off for 4 ms while its discharge capacitors are being charged. After the 4 ms delay, the laser sends out an external trigger signal and pulses the laser chamber.

This 4 ms delay is outside the range for the camera system to accept as valid. The circuit shown in fig. 2.4 solves this problem by delaying the laser's external trigger until the next camera TRIG OUT signal is received. With this scheme the camera frame in which the laser pulse occurs is read out and discarded since the TRIG IN signal is not received until the next TRIG OUT signal is sent. The camera has an inject inhibit signal which prevents the pixels from being scanned. The inject inhibit signal is held true between the first and second TRIG OUT signals and then released. The camera system then takes the second frame as valid and stores it in memory.

2. Multiple Pulse Integration

The circuit in fig. 2.4 also has the capability of integrating multiple pulses onto the camera. The counting chips in the circuit count the number of incoming laser pulses and compare this to the number set by the eight dip switches. When the pulse total reaches the set limit, the inject inhibit is released and the camera is sent a TRIG IN signal.

A maximum of 255 pulses can be integrated onto the camera. At the laser's max-

imum repetition rate the camera must integrate for approximately one second. This integration time is 72 times longer than a standard camera frame. This long integration time leads to problems with background light. Proper shielding must be used to prevent the build up of background light.